Global Value Chains Drive Disparities in the Health Consequences of Shipping*

Richard Klotz† and Rishi Sharma‡

April 2025

Abstract

Despite a growing awareness of the health burdens associated with the local air pollution emissions from shipping, responsibility for these burdens is not well understood. Here we quantify the country-level contributions and exposure to the fine particulate matter ($PM_{2.5}$) mortality impacts of shipping across global value chains using top-down accounting and input-output methods. Our analysis reveals stark disparities in contributions and exposure to shipping related mortality. High income countries bear less than 10% of mortality while contributing over 35%. For the median country, over 95% of shipping related mortality is not associated with their own consumption or production. Global value chains serve as a key driver of these disparities by amplifying the exposure at certain locations of the global shipping network while also moderating the non-income determinants of contributions.

*This paper utilized the Colgate Supercomputer, which is partially supported by NSF grant OAC-2346664.

†Department of Economics, Colgate University (rklotz@colgate.edu)

‡Department of Economics, Colgate University

1 Introduction

The growth of global value chains (GVCs) has increased the spatial fragmentation of production, such that final consumption is connected through global trade to multiple stages of production across many countries [1, 2, 3]. An important environmental concern related to GVCs is that fragmented production can potentially shift exposure to environmental hazards from production onto populations that do not ultimately benefit from the goods being produced [4, 5]. The growth of GVCs is also associated with the increased movement of goods, and despite considerable research on the aggregate health burden of shipping [6, 7, 8], disparities in exposure and contributions to this burden have remained unexplored. Here we quantify the country-level contributions and exposure to the fine particulate matter ($PM_{2.5}$) mortality impacts of shipping across global value chains using top-down accounting and input-output methods. Our analysis reveals stark disparities in contributions and exposure to shipping related mortality. High income countries bear less than 10% of mortality while contributing almost 35%. For the median country, over 95% of shipping related mortality is not associated with their own consumption *or* production – a characteristic that distinguishes shipping emissions from production emissions [5]. GVCs serve as a key driver of these disparities by amplifying the exposure in the vicinity of major global shipping lanes while also moderating the non-income determinants of contributions. GVC linkages also effectively "conceal" the relationship between consumption and mortality, with for example the consumption of non-traded goods accounting for 40% of shipping mortality. The interplay between consumption, GVCs and shipping has important consequences for the distributional effects of local and global policies to regulate local pollutants from shipping, maritime decarbonization, trends in the use – and therefore shipping of fossil fuels – and "reshoring."

Prior to recent policy actions, shipping has been estimated to cause 60-400 thousand premature deaths each year [8]. The vast majority of these deaths result from elevated fine particulate matter ($PM_{2.5}$) in coastal areas due to the combustion of maritime distillate and residual fuels, which contributes both primary $PM_{2.5}$ and secondarily formed $PM_{2.5}$ due to emissions of sulfur and nitrogen oxides (SOx and NOx). The challenges in attributing mortality from shipping to final activities (i.e., consumption) are that shipping takes place between every stage of production and across a global shipping network – with over 80% of goods by weight traveling on ocean going vessels [9] – and that the health impacts of emissions from ships vary substantially across space depending on the proximity to human populations and the chemical transport of pollutants. For example, the purchase of a Japanese built car in Europe would contribute to health impacts due to the shipping of the car from Japan

to Europe (perhaps through Antwerp). This shipping would contribute to air pollution and mortality in Japan and Europe, as well countries close to shipping routes through the South China, Red and Mediterranean seas, and the Indian Ocean. But shipping is also used to move parts to Japan, perhaps from countries in South Asia, and the raw materials used to make these parts (e.g., minerals from Australia or oil from the Middle East), and so on. Quantifying how consumption contributes to the health impacts associated with shipping therefore requires linking data on all bilateral trade flows to estimates of mortality from shipping on each trade flow that depend on the ports and routes used, the characteristics of vessels and how emissions along the shipping network affect mortality.

A number of previous studies have linked production emissions to consumption using input-output methods, initially focusing on greenhouse gases (GHGs) [10, 11]. These studies emphasize that due to the GHGs embodied in trade there are important differences in accounting for emissions based on the location of release as opposed to the consumption ultimately being supported. Studies that extended these methods to local pollutants have especially highlighted how exposure to pollution disproportionately falls on regions [12, 4, 5, 13, 14, 15] and sociodemographic groups [16, 17] that are not the final consumers. For example, Zhang et al. [5] shows that 22% of global mortality related to $PM_{2.5}$ from the production of goods is associated with consumption in other regions. Despite shipping's important contribution to air pollution and the possibility for starker disparities because shipping activities can occur far from the producers and consumers of goods being shipped, none of these studies focus on shipping and often exclude international transportation from the analysis. A number of the recent studies on the environmental impacts of shipping have used bottom-up approaches based on Automatic Identification System (AIS) data to estimate the contribution of shipping to local pollutant emissions and health impacts at the global [8, 18, 19] or regional scale [20, 21]. These studies have highlighted disparities in exposure to emissions from shipping, but since they do not link shipping activities to trade flows, the impacts of these emissions cannot be attributed to consumption. Studies that do link shipping activities to trade flows have only done so for specific bilateral flows and have not considered multiple stages of production [22, 23], or have not linked emissions to consumption (and focused on GHGs) [24, 25].

Here we quantify the disparities in contributions and exposure to the health impacts of shipping across global value chains using a top-down accounting of the $PM_{2.5}$ related mortality impacts of shipping and input-output methods. The top-down accounting combines the first estimates of the marginal mortality from shipping – the number of deaths (by country) per dollar for each trade flow (country pair by sector) – with a multi-region input-output database. To construct the marginal mortality estimates, we first use a global

database of vessel port calls and global trade data to calculate how a dollar of a good moving between two countries contributes to weight shipped by vessel type between port pairs. Next, we use routing models, vessel characteristics and emissions factors to allocate the port-to-port flows to fuel use and emissions on links in a global maritime network. The routing models allow us to capture differential behavior across vessel types, in particular the indirect shipping and transhipment at hub ports of containerized goods [26]. Finally, we use a source-receptor matrix constructed using a reduced complexity air pollution model and standard concentration-response functions to calculate how the emissions (on the network) contribute to mortality in each country. Using input-output methods we calculate how each country's final consumption contributes to shipping related mortality in each other country, across all production stages, and the disparity in exposure and contributions to mortality. To investigate the role of GVCs, we decompose contributions by production stage (shipping final goods, direct inputs, inputs-to-inputs, etc.) and exposure into mortality related to own-country activities and activities in other countries. A full description of our methods are available in the Supplemental Material.

2 Results

Global Totals Table 1 reports our top-down estimates of shipping activities, emissions and shipping-related mortality. In our main analysis, we assume that the fuel sulfur limits designated by the International Maritime Organization (IMO) in place at the end of 2020 – 0.5% fuel sulfur by weight globally due to a regulation referred to as IMO 2020 and 0.1% in Emission Control Areas (ECAs) off the coast of North America and in the North and Baltic seas – are binding. The estimated annual value of goods carried by ships, for domestic (or coastal) and international shipping, is over $20 trillion (in 2017 US dollars) and the weight carried by ships is 25.7 billion tons. Shipping services total 118 trillion ton-kilometers, require 233 million tons of fuel and results in the emission of 0.52 million tons of primary $PM_{2.5}$, 2.08 tons of SO_x and 21.53 tons of NO_x. The mortality due to elevated ambient $PM_{2.5}$ resulting from these emissions are over 205,000 deaths per year. This is a lower-bound of the overall health impacts of shipping because vessels also release other pollutants (e.g. VOCs), and ambient $PM_{2.5}$ also contributes to other negative health impacts including morbidity [27]. These estimates of fuel use, emissions, and mortality are broadly to comparable global statistics [9] and, in the case of emissions and mortality, inventory studies of the local pollution impacts from shipping that use similar assumptions [8, 19] (see Section B in the Supplemental Material).

Exposure and Contributions to Mortality Panel (a) in Figure 1 shows each country's per capita exposure to shipping related mortality. Mortality is concentrated along the major shipping lanes connecting Europe and Asia, with high levels across the Mediterranean, Red Sea, Indian Ocean and South and East China Seas. For example, mortality per million people is 24.0 in Egypt, 20.2 in Tunisia, 16.9 in India, 32.1 in Japan and 51.3 in Sri Lanka, compared to a global median of 8.8. The shipping traffic contributing to mortality does not originate and is not destined for many of these highly exposed countries. By contrast, mortality is quite low in North America (e.g. 7.9 in US), Northern Europe (e.g. 11.2 in UK, 12.4 in Germany) and Australia (2.4), which are distant from major shipping lanes and/or are partially protected by ECAs.

Panel (b) of Figure 1 shows the per capita contributions to global mortality due to shipping on the basis of consumption. The spatial distribution of contributions is strikingly different from the distribution of exposure in the first panel. Countries with high per capita income tend to have the highest contributions to mortality. Contributions to mortality per million people are 52.5 for the US, 40.9 for Germany, 117.0 for Bahrain and 72.5 for Japan compared to a global median of 17.6. The median low income country contributes just 10.2 deaths per million people.

The first two panels of Figure 1 are suggestive of the disparity between countries' contribution and exposure to mortality. A more direct metric for this disparity is the ratio of a country's exposure to shipping mortality to its contribution to shipping mortality (c.f. the pollution inequity measure used by [16] in the context of US consumption). A value of 1 would mean that a country's per capita exposure is equal to its per capita contribution. The median country is exposed to 0.44 deaths for each death it contributes. Panel (c) of 1 shows that this exposure-contribution ratio varies starkly across the world, with almost all rich countries below the median contribution-exposure ratio and most lower income countries above it. North America and Northern Europe have values that are close to 0 (e.g. 0.15 in the US, 0.13 in Canada, 0.30 in Germany). Relatively lower income countries near major shipping lanes in general tend to experience very high exposure relative to contributions. For example, China is exposed to 1.70 deaths for each death it contributes, Vietnam to 2.27, Sri Lanka to 2.51, Colombia to 3.57 and Ethiopia to 3.74.

Exposure to Activities of Other Countries The patterns in exposure and contributions indicate that much of the exposure countries face is the result of activities of other countries. As shown in the Supplemental Material, we can calculate the contribution of other countries' activities to exposure in each country by stripping out mortality related to own country consumption and own country participation in other countries' value chains

(in the sense of being an importer or exporter of goods ultimately supporting consumption in other countries). We find that activities in other countries account for about 46% of total global mortality (Table 2). Own consumption and contributions to the supply chains of other countries are 37% and 17%, respectively. Due to the substantial own country contributions of India and China, the effect is even more stark for the median country: in the median country 96% of mortality is unrelated to own consumption and value chain contributions. The pervasiveness of exposure to activities of other countries is a distinctive characteristic of the health impacts of shipping. Unlike in the production emissions context ([12, 4, 5]), exposure to shipping emissions occurs due to the routing of vessels through the global shipping network.

At the country level (Figure A.1), larger economies tend to mainly bear more mortality from their own activities, either due to consumption, or production of raw materials or intermediates, while countries with smaller economies tend to bear more mortality from activities they are uninvolved in. For example, mortality from other countries' activities is lowest in the US, China, Brazil and Australia. India is somewhat of an outlier – a large economy with a relatively large share of mortality from other's activities – due to its position between China and Europe. Using mortality due to other countries' activities in the exposure-contribution ratio (Figure A.2) does not drastically alter the spatial patterns in disparities discussed above. However, larger economies tend to have lower exposure-contribution ratios in this case due to the importance of own activities for these countries.

Exposure and Contributions of Mortality Across Income Groups and Regions Our methodology allows us understand how value chains link consumption in each country to mortality in every other country. The left side of Figure 2 depicts these results aggregated to income brackets. The left most bar depicts mortality by income bracket, while the next bar to the right depicts the income brackets whose consumption is ultimately responsible for this mortality. There is again a clear disparity between exposure and contributions: High income countries bear less than 10% of shipping related mortality, while contributing 34%. In contrast, lower income countries bear around 26% of mortality from shipping, while contributing around 21%, and middle income countries bear around 64% and contribute around 45%. Apart from the disparity in exposure and contributions, we also see a clear shifting of environmental burden: high income countries contribute almost 19,000 deaths in lower income countries. Lower income countries, however, contribute only around 1,800 deaths in high income countries.

The right side of Figure 2 depicts total mortality and the contributions to mortality from shipping by region. As shown by the earlier maps, the majority of exposure to mortality

is in Asia and the Middle East and North Africa (MENA) due to their close proximity to busy shipping lanes. Europe, North and South America experience relatively little mortality, especially considering the size of these economies. The most notable pattern in the flows of mortality between regions is that other-region consumption contributes little to mortality in North America (1,188 deaths) and Europe (6,135 deaths), compared to Asia (48,226 deaths), MENA (5,976 deaths) and Sub-Saharan Africa (1,882 deaths).

Panel (b) of Figure 2 expands the left side of Panel (a) to illustrate how they types of goods being consumed (third column) and being shipped (second column) mediates the exposure and contributions patterns across countries. Among the shipped goods, fossil fuel shipping in particular is notable with the shipping of petroleum, natural gas and coal accounting for almost 35% of total global mortality from shipping. This highlights the important role of the mere shipping of fossil fuels in generating local pollutant damage.

While the shipping of fossil fuels and other primarily intermediate input sectors such as chemicals and mining/metal dominate the mortality contributions, the consumption goods that ultimately drive this shipping are quite different. Consumption of services account for 41% of global deaths despite technically being a mostly non-traded sector – a fact that highlights the importance of accounting for value chain linkages. Examining the sectoral and income patterns together, it is clear that richer countries consumption of these ostensibly cleaner goods drive a substantial portion of mortality. It is also notable that food consumption accounts for a larger share of mortality contributed for low and middle income countries than for high income countries.

Key Role of Global Value Chains Figure 2 indirectly points to the fact that global value chains are a key driver of the disparities in the exposure and contribution to shipping-related mortality. Analyzing mortality by production stage – stage 0 is the shipping of final goods, stage 1 is the shipping of inputs to the production of final goods, stage 2 is the shipping of inputs to inputs, and so on – reveals that value chains amplify exposure in countries near shipping lanes while weakening non-income determinants of contributions.

The mortality embodied in the trade flows between Germany and the US and China and the US are mapped by production stage in Figures 3 and 4. The Germany–US maps illustrate that with global value chains even highly regional activities contribute heavily to mortality in the regions most exposed to shipping lanes due to the shipping of inputs embodied in these activities. Mortality associated with stage 0 (panel (a)) – the direct shipping of goods from Germany to the US – is mainly in the countries along the shipping lanes connecting the two trade partners (e.g., US, Germany and the countries in northern Europe and Caribbean). However, when moving back through the stages of the supply chain,

shipping mortality concentrates in Asia/Pacific (China and India especially) and in north Africa and the Middle East, despite these areas being quite distant from the shipping lanes between US and Germany. After accounting for all production stages (stage ∞) overall mortality in these regions easily exceed the mortality in the US or Germany. The most notable pattern for the China–US trade flow is that mortality in China increases substantially as more production stages are included. Since China is central to global supply chains and shipping networks, going back through the supply chain amplifies shipping activity and mortality in and around China.

Value chains concentrating mortality in certain regions is clearly evident at more aggregate levels, indicating that this effect is systematic. Figure 5 plots regional contributions (from consumption) to regional mortality by production stage. Across all regions, a sizable fraction of stage 0 mortality is within the contributing region. However, overall mortality tends to be dominated by contributions to the highly exposed regions (largely MENA and Asia/Pacific) in stage 1 and beyond. This pattern is especially clear for North America and Europe. For example, the majority of North American contributions to mortality occur in Asia/Pacific and MENA, but only a small fraction of this mortality is related to the shipping of final goods. This amplification of mortality is also evident for Asia/Pacific, where contributions to mortality are nearly all in the same region, but about 80% of overall contributions are due to value chains.

Unlike exposure, the maps in Figure 1 indicate that contributions to mortality are driven primarily by GDP per capita. To understand this pattern, note that per capita contributions to mortality is the product of income per capita and mortality per dollar of consumption. Therefore, a 1% increase in income would be associated with a 1% increase in mortality per capita unless there are also differences in mortality per dollar of consumption, which captures the non-income related determinants of contributions to mortality such as geography, transportation infrastructure and consumption patterns. To explore these relationships, in Table 3 we present slope coefficients of bi-variate regressions of (logged) per capita contributions to mortality and other determinants of per capita contributions to mortality on (logged) per capita income at the country level. We estimate these regressions for each outcome in stage 0 (first column of numbers) and when the outcome is accumulated over further production stages (remaining columns) to show the contributions of value chains.

For stage 0, a 1% increase in per capita income is associated with a 0.49% increase in per capita contributions to mortality and per capita income explains only 31% of the variation in per capita contributions (first row). This shows that for direct shipping, non-income related differences across countries play an important role in the relationship between income and contributions. Mortality per dollar of consumption (second row) falls with income because

lower income countries are more dependent on shipping by sea ($ shipped by sea per dollar of consumption) and on shipping services (kg-km per dollar shipped), which are both connected to the geographic and structural features of countries.

When considering contributions to mortality across the entire value chain, however, the relationship between income and contributions becomes substantially stronger; a 1% increase in income is associated with a 0.73% increase in mortality and income explains 74% of the variation in per capita contributions. Countries' non-income determinants of mortality are averaged out over the value chain (mortality per dollar falls) because the shipping of intermediate inputs is concentrated in major shipping lanes regardless of the ultimate location of final consumption.

Impacts of Recent Policy Actions Recent policy actions have targeted maritime fuel sulfur at the global and local scale and have dramatically changed the health implications of shipping. IMO 2020 reduced the global fuel sulfur limit from 3.5% to 0.5%, while ECAs limited fuel sulfur to 0.1% in the North and Baltic Sea, and within 200nm the coast of the US and Canada (North American ECA). Table 4 illustrates how these policies have altered contributions and exposure by income group. Absent these policies, mortality associated with shipping would be over 375,000 deaths per year. Likewise, across income bracket and region, contributions and exposures would have been substantially higher. For example, consumption by high income countries would contribute about 37,500 deaths in the lowest income countries.

The ECAs have a relatively minor impact on the overall mortality (a reduction in mortality of roughly 9,100 deaths). Although vessel responses to the ECAs can somewhat undercut the reductions in mortality [28], here we assume vessel behavior is fixed. Due to their locations, these ECAs almost exclusively reduce mortality in high income countries and mainly from mortality related to consumption in these high income countries. Almost 70% of the overall reduction in mortality from ECAs is contributions of high income countries to mortality in other high income countries.

The global fuel sulfur limits imposed by IMO 2020 are much more consequential, with over 170,000 lives saved. Because this policy reduces contributions and exposure in a roughly proportional manner, in an absolute sense this has the largest impacts on across country contributions, which tend to affect low income countries. Overall, IMO 2020 reduced high and middle income countries' contributions to mortality in low income countries by almost 32,000 (19,000 + 13,000) deaths per year. These IMO 2020 results provide a strong illustration of a key theme in the environmental justice literature: broad regulations that reduce environmental damage – even through a uniform policy – tend to reduce pre-existing

environmental inequities [29].

Sensitivity Analysis Uncertainties in our estimates of exposure and contributions arise from both the economic data used to construct the input-output matrix and the measurement of the marginal mortality from shipping. Like other studies of this type, we are limited in our ability to explore the uncertainties in the economic data because most global input-output datasets, including the one used here, do not report uncertainties in the economic statistics. However previous research – in the context of greenhouse gas emissions – suggests that the main source of uncertainties is in the emissions calculations as opposed to the input-output data [30, 31]. We therefore explore the sensitivity of exposure and contributions due to key assumptions in the marginal mortality of shipping.

Table 5 illustrates that while the estimates of total mortality due to shipping depend heavily on parameter assumptions, the relative contributions of regions to mortality in other regions are relatively insensitive. The first row presents our central results with IMO 2020 in place. The next four rows display results using alternative calibrations of the concentration-response function used in the literature (see Section A in the Supplemental Material). The next two rows display results using upper and lower baseline mortality rates from Across these assumptions, our estimates of total mortality range from 106,000 to 308,000, but the relative contributions of regions to mortality in other regions are essentially unchanged. The remaining columns report results using different assumptions about vessel technologies. Using global average fuel economy (tons fuel per kg-km) estimates by vessel type from [24] or [19] illustrates the important trends in vessel fuel efficiency over the last decade and shows that the spatial distribution of vessel technology – which is captured in our central results – does not play a key role in the distribution of mortality. The final set of results – which forces containerized goods to travel on minimum distance routes while assuming global average fuel economy from [19] – illustrates that indirect container shipments have an important impact on global mortality, roughly 13,000 deaths.

3 Discussion

Using newly constructed estimates of the marginal mortality from shipping and input-output methods, we quantify the disparities in contributions and exposure to the air pollution related mortality impacts of shipping, accounting carefully for the role of global value chains. We find that high income countries bear less than 10% of mortality while contributing almost 35%. For the median country, over 95% of shipping related mortality is not associated with their own consumption production. Consumption in upper and middle income countries

contributes to over 40,000 shipping related deaths per year in low income countries with current policies. Prior to IMO 2020, this transfer was much larger at over 82,000 deaths per year.

Global value chains are a key driver of the observed disparities. GVCs both concentrate mortality in countries close to major shipping lanes, and spread the impacts of countries' consumption across the world so that income – as opposed to non-income factors – primarily determines contributions to mortality. Both of these factors ultimately amplify the disparities in exposure and contributions to shipping related mortality. We show that the mortality embodied in trade, across all productions stages, is both much larger and more geographically distant from final consumption than if only the direct flows are considered (as in [23]). For example, only 15% of the mortality from China to US trade is a result of the direct flows. Studies based on vessel inventories – and not trade flows – are not able to reveal these patterns. Moreover, methods for attributing responsibility for shipping mortality without accounting for value chains – such as those based on origin or destination country or location of the bunker purchase as suggested by the UNFCCC in the context of GHGs [32] – will misrepresent the disparities in exposure and contributions. In particular, the contribution of lower income countries will be overstated (and those of higher income countries understated) since much of the shipping to/from lower income countries actually serves the supply chains for richer countries (Table A.2).

From a policy perspective, our results provide some guidance for addressing the disparities in the health consequences in global shipping. Further tightening the sulfur limit beyond IMO 2020 would reduce disparities in an absolute sense, but with unknown and potentially large costs. While current ECAs targeting sulfur have tended to protect higher income countries, establishing similar ECAs in the most heavily trafficked or highest mortality areas – like the Mediterranean Sea– would not only reduce aggregate mortality but would weaken the disparities across income groups (Table A.3). With IMO 2020 in place, efforts to reduce shipping related mortality might be better focused on NOx. NO_x ECAs could – depending on the technology used for compliance – impact mortality across broader areas than sulfur ECAs because compliant vessels would generate less NOx along their entire voyage and non-compliant vessels might shift to unregulated routes. However, there is skepticism about the efficacy of NO_x ECAs as currently implemented [33].

Our results also inform current discussions related to the decarbonization of maritime transport. A full decarbonization would likely provide both substantial health co-benefits – since low carbon technologies also tend to contribute less to particulate matter – and mostly eliminate the disparities across income groups and geography. The health impacts of proposed "green corridors," which aim to decarbonize specific shipping lanes [34], are much

less clear. If the regulated lane does not occupy a central position in value chains (e.g. it is primarily moving raw materials or final goods), then these types of policies may prevent only a relatively small fraction of the total mortality, or GHG emissions, generated by the underlying trade between the countries involved.

Given our finding that the shipping of fossil fuels accounts for 35% of global shipping mortality, even broader climate actions – like improvements in the energy efficiency of production – could generate meaningful reductions in mortality due to shipping. Reducing energy inputs per dollar of output by 25% for all production sectors globally, holding all else equal, leads to a reduction of over 15,000 deaths from shipping with most of these reductions in low and middle income countries (Table A.4). These effects, though large, are likely to be considerably smaller than the mortality impacts of reduced fossil fuel use in production.

More general economic trends that alter supply chains – such as the relocation of production activities to firms' home countries [35] or "reshoring" – will also impact mortality related to shipping. Reducing the share foreign goods in both production and consumption in the US by 25% (and scaling domestic goods accordingly) would lead to a reduction of about 3,500 deaths globally (Table A.4). This reduction in mortality occurs mainly in low and middle income countries, but is almost exclusively linked to in consumption higher income countries (the US and its close trading partners). A similar reshoring counterfactual for China would also lead to about 3,500 fewer deaths, though a larger share of this reduction is linked to other country consumption due to China's central role in global value chains. This analysis is only a rough accounting of reshoring scenarios because it does not account for market adjustments or changes in mortality linked to production or other transportation modes.

4 Methods

Our analysis relies on a global top-down accounting of shipping mortality that links trade flows – quantities of goods moving between and within countries – to trade flow specific estimates of the marginal mortality – deaths associated with the shipping of a unit of goods. Other examinations of shipping related mortality have used bottom-up methods based on detailed vessel activity data [21, 8], or assessed a single trade flow [23]. Our approach enables us to quantify the mortality associated with all trade flows, and to attribute shipping related mortality to final consumption. A full exposition of our modeling framework and data are available in the Supplemental Material.

4.1 Top-Down Accounting of Mortality from Shipping

In the top-down accounting we consider N countries and S sectors.The trade flows, x_{ij}^{st}, are the purchases of good s from country i used by sector t in country j, and $X = \{x_{ij}^{st}\}$. Final demand is Y_i^s, so total output for each sector is $X_i^s = \sum_{jt} x_{ij}^{st} + Y_i^s$ or in vector form X_{tot} The multiregion input-output (MRIO) matrix $A = \{a_{ij}^{st}\} = X * diag(1/X_{tot})$ describes the dollars of good s from country i used by sector t in country j.

The marginal mortality in country k from moving a dollar of good is to jt are d_{ijk}^{st}. These measures map a dollar of each trade flow to a quantity and geographic distribution of emissions produced – which depends on the vessels, ports and routes used – then link these emissions to country-specific mortality accounting for the physical transport of the pollutants and the location of population. Marginal mortality is calculated as:

$$d_{ijk}^{st} = s_{ij}^{s} * wv_{ij}^{s} * \sum_{ode} \theta_{ijod}^{s} * \pi_{ode}^{s} * m_{odek}^{s} \tag{1}$$

where s_{ij}^s is the share of each trade flow that travels by sea and wv_{ij}^s is the weight-to-value ratio for good s produced in country i and imported by j. θ_{ijod}^s is the share of good s shipped from i to j that travels between ports o and d and π_{ode}^s is the probability that vessels carrying good s from port o to port d use edge e of the maritime network. Finally, m_{odek}^s is the mortality in country k associated with moving a ton of good s between port o and d on edge e of the maritime network. Note that the damage matrix does not vary with using sector t (i.e., $d_{ijk}^{st} = d_{ijk}^{s}$).

Global mortality from shipping in country k is therefore $\sum_{ij,st} d_{ijk}^{st} * x_{ij}^{st}$. Mortality related to a country's imports, exports, or a particular trade flow could be calculated similarly after zeroing out the appropriate elements of x.

4.2 Attributing shipping mortality to final consumption

Given our top-down accounting, we can use input-output methods to calculate the shipping mortality associated with final consumption. Input-output methods are often used to measure supply chains [36] and to quantify the environmental impacts embodied in consumption [37, 10] and trade [12, 5], but have never been applied to air pollution from shipping.

Given the input-output matrix, the Leontief inverse matrix can be calculated as $L = A^0 + A^1 + A^2 + \ldots = (I - A)^{-1}$ The powers of A denote the inputs required to produce each good at the production stage given by the power (so $A^1 = A$ are the inputs used to produce each good, and A^2 are the inputs used to produce the inputs of each good). Therefore, the

elements of L contain the additional units of each good that are needed – at any production stage – to produce a unit of each good.

The N by $N * S$ matrix $D = \{\sum_{is} a_{ij}^{st} * d_{ijk}^{st}\}$ contains the mortality in each country k (rows) associated with the shipping of all inputs used to produce a unit of good jt. For example, if shipping a dollar of output from sector 1 to sector 2 causes 1 death, and the production of a dollar in sector 2 requires 0.5 dollars of goods from sector 1, then the total mortality from shipping inputs to sector 2 are 0.5.

The mortality in each country from the consumption of a dollar of each good in each country can be calculated as $\tilde{d} = DL$. Therefore, the total mortality (in each country) associated with the consumption of each country can be calculated as $\tilde{D} = DLY$, where Y is a $N * S$ by N matrix with the rows representing the final consumption vectors of each country and $\tilde{D}$ is an N by N matrix. A^n can be substituted for L in these equations to obtain the mortality vectors for production stage n.

Contributions to mortality of bilateral tradeflows are calculated by adding columns to the MRIO (and corresponding rows of zeros). The elements of the columns are the dollars of good s from country i that moves to country j, either as an intermediate input or for consumption, per dollar of total trade between country i and j. The corresponding elements in A therefore represents the goods embodied in each trade flow.

We decompose a country's exposure to mortality as $D_k = \tilde{D}_k^{own} + \tilde{D}_k^{mx} + D_k^{un}$ or the sum of mortality due to own country consumption, due to imports and exports to the country that are ultimately embodied in other countries' consumption, and due to activities unrelated to country k. D_k are the row sums of $\tilde{D}$. and D_k^{own} are the diagonal elements of $\tilde{D}$. D_k^{mx} can be calculated as the row sum of the off-diagonal elements of $\tilde{D}^{mx}$, where $\tilde{D}^{mx}$ is calculated in the same manner as $\tilde{D}$ but after zeroing out the marginal mortality for countries other than the importing and exporting countries in d_{ijk}^{st} (that is where $i \neq k$ or $j \neq k$). Third party related mortality can be calculated as $D_k^{third} = D_k - \tilde{D}_k^{own} - \tilde{D}_k^{IJ}$. Note that a similar decomposition can be done for contributions, D_i, but in this case the third-party term would be a country's contribution to mortality in countries that do not contribute to the value chains utilized by country i.

4.3 Data

MRIO Matrix The MRIO is obtained from the Global Trade Analysis Project (GTAP) 11B database [38]. We use the 2017 reference year and aggregate to 20 sectors and 129 countries/regions (see Supplemental Material).

Sea Shares and Weight to Value Ratios Sea shares are constructed from 2018 data from the UN Comtrade database [39]. We use 2018 data to maximize geographic coverage, while still avoiding the pandemic affected years starting in 2019. We calculate sea shares for our region and sector definitions after assigning any road and rail flows to sea if a land route between the trading partners is unlikely. This adjustment corrects for Comtrade reporting the mode on which goods leave the country as opposed to its longest leg. Domestic shares are constructed using average mode shares between a country and its contiguous trading partners if those contiguous partners total at least 5% of total trade. We fill in missing shares using the reverse bilateral pair, or subregional/regional averages.

Weight-to-value ratios are constructed at the country-pair by sector level from the 2018 BACI product-level trade database [40].

Port Shares There are no global databases of trade flows at the port level. Following previous studies [23, 41, 26], we obtain θ^s_{ijod} mainly from a global dataset of port calls purchased from Astra Paging. For non-containerized goods, we calculate the weight of goods moved between ports using the vessel calls data, and use these flows to calculate port shares. We use an vessel inventory model to calculate port-to-port flows of goods to account for the possibility that bulkers and tankers may lade and unlade at multiple ports. For the country pairs that we do not observe port flows (including containerized goods) we assign port shares proportionally to the total weight of goods arriving/departing at each port-pair.

Edge Probabilities The edge probabilities allocate vessels moving between two ports to edges of a maritime network. Our maritime network is from Eurostat's SeaRoute program but has been updated to better reflect observed vessel routes. The edge probabilities capture differential routing behavior across vessel types, which plays a role in the distribution of shipping activities and emissions. Tankers, bulk carriers and other cargo ships mostly operate on flexible, non-scheduled routes moving goods directly between origin and destination ports [41]. We therefore assume that this set of ships takes the minimum distance route between port pairs. Container ships typically offer liner service (scheduled, fixed routes) using a hub-and-spoke model, where goods are moved are transshipped from smaller ports to hubs, then between hubs, before finally moving to the destination port [26]. We capture the indirect shipping and transhipment behavior by calibrating a routing model to match observed vessel traffic [42, 26].

Edge Mortality We link shipping emissions to mortality using source-receptor (SR) matrices that described the increased mortality (in each country) associated with one ton

of pollution ($PM_2 \cdot 5$, SO_x and NO_x) emitted at each cell of a grid that covers the maritime network. Source-receptor matrices are used in a range of studies [43, 44, 45] and this approach – as opposed to simulating mortality associated with emissions on each link of the network – greatly reduces the computational burden of estimating mortality. Mortality associated with the movement of a ton of goods on each edge in the maritime network is the sum across all grid cells of the emissions released in each cell on that edge – distance traveled in the grid cell times a good specific fuel use factor (fuel user per unit of shipping) times an emissions factor – multiplied by the mortality due to a ton of pollution emitted in that cell from the SR matrices. The SR matrices were constructed using a global version of InMap [46, 47]. The resolution of the matrices – grid cells in the open ocean are 5° by 4°, while cells intersect land are 2.5° by 2° – broadly matches the computational grid used in [47]. In our main results we consider the cardiovascular and lung cancer related mortality associated with elevated $PM_{2.5}$ using log-linear relative response functions parametrized to be consistent with [8] and baseline cause-specific mortality rates from [48]. We also generate results with the high and low parameter estimates from [8] and with two other commonly used parameter estimates [49, 50].

References

[1] Robert C. Feenstra. Integration of Trade and Disintegration of Production in the Global Economy. *Journal of Economic Perspectives*, 12(4):31–50, 1998.

[2] Robert C. Johnson and Guillermo Noguera. Accounting for Intermediates: Production Sharing and Trade in Value Added. *Journal of International Economics*, 86(2):224–236, 2012.

[3] Robert C. Johnson and Guillermo Noguera. A Portrait of Trade in Value-Added over Four Decades. *The Review of Economics and Statistics*, 99(5):896–911, 2017.

[4] Azusa Oita, Arunima Malik, Keiichiro Kanemoto, Arne Geschke, Shota Nishijima, and Manfred Lenzen. Substantial Nitrogen Pollution Embedded in International Trade. *Nature Geoscience*, 9(2):111–115, 2016.

[5] Qiang Zhang, Xujia Jiang, Dan Tong, Steven J. Davis, Hongyan Zhao, Guannan Geng, Tong Feng, Bo Zheng, Zifeng Lu, David G. Streets, Ruijing Ni, Michael Brauer, Aaron van Donkelaar, Randall V. Martin, Hong Huo, Zhu Liu, Da Pan, Haidong Kan, Yingying Yan, Jintai Lin, Kebin He, and Dabo Guan. Transboundary Health Impacts of Transported Global Air Pollution and International Trade. *Nature*, 543(7647):705–709, 2017.

[6] Kevin Capaldo, James J. Corbett, Prasad Kasibhatla, Paul Fischbeck, and Spyros N. Pandis. Effects of Ship Emissions on Sulphur Cycling and Radiative Climate Forcing Over the Ocean. *Nature*, 400(6746):743–746, 1999.

[7] James J. Corbett, James J. Winebrake, Erin H. Green, Prasad Kasibhatla, Veronika Eyring, and Axel Lauer. Mortality from Ship Emissions: A Global Assessment. *Environmental Science & Technology*, 41(24):8512–8518, 2007.

[8] Mikhail Sofiev, James J. Winebrake, Lasse Johansson, Edward W. Carr, Marje Prank, Joana Soares, Julius Vira, et al. Cleaner Fuels for Ships Provide Public Health Benefits with Climate Tradeoffs. *Nature Communications*, 9(1):1–12, 2018.

[9] UNCTAD. *Review of Maritime Transport, 2018*. United Nations Conference on Trade and Development (UNCTAD), Geneva, Switzerland, 2018.

[10] S. J. Davis and K. Caldeira. Consumption-Based Accounting of CO2 Emissions. *Proceedings of the National Academy of Sciences*, 107(12):5687–5692, 2010.

[11] Steven J. Davis, Glen P. Peters, and Ken Caldeira. The Supply Chain of CO2 Emissions. *Proceedings of the National Academy of Sciences*, 108(45):18554–18559, 2011.

[12] Jintai Lin, Da Pan, Steven J. Davis, Qiang Zhang, Kebin He, Can Wang, David G. Streets, Donald J. Wuebbles, and Dabo Guan. China's International Trade and Air Pollution in the United States. *Proceedings of the National Academy of Sciences*, 111(5):1736–1741, 2014.

[13] Haikun Wang, Yanxu Zhang, Hongyan Zhao, Xi Lu, Yanxia Zhang, Weimo Zhu, Chris P. Nielsen, Xin Li, Qiang Zhang, Jun Bi, and Michael B. McElroy. Trade-Driven Relocation of Air Pollution and Health Impacts in China. *Nature Communications*, 8(1):1–7, 2017.

[14] Keisuke Nansai, Susumu Tohno, Satoru Chatani, Keiichiro Kanemoto, Midori Kurogi, Yuta Fujii, Shigemi Kagawa, Yasushi Kondo, Fumiya Nagashima, Wataru Takayanagi, and Manfred Lenzen. Affluent Countries Inflict Inequitable Mortality and Economic Loss on Asia Via PM2.5 Emissions. *Environment International*, 134:105238, 2020.

[15] Guangxiao Hu, Kuishuang Feng, Laixiang Sun, and Giovanni Baiocchi. Tracing Toxic Chemical Releases Embodied in U.S. Interstate Trade and Their Unequal Distribution. *Environment International*, 171:107681, 2023.

[16] Christopher W. Tessum, Joshua S. Apte, Andrew L. Goodkind, Nicholas Z. Muller, Kimberley A. Mullins, David A. Paolella, Stephen Polasky, Nathaniel P. Springer, Sumil K. Thakrar, Julian D. Marshall, and Jason D. Hill. Inequity in Consumption of Goods and Services Adds to Racial–Ethnic Disparities in Air Pollution Exposure. *Proceedings of the National Academy of Sciences*, 116(13):6001–6006, 2019.

[17] Narasimha D. Rao, Gregor Kiesewetter, Jihoon Min, Shonali Pachauri, and Fabian Wagner. Household Contributions to and Impacts from Air Pollution in India. *Nature Sustainability*, 4(10):859–867, 2021.

[18] Lasse Johansson, Jukka-Pekka Jalkanen, and Jaakko Kukkonen. Global Assessment of Shipping Emissions in 2015 on a High Spatial and Temporal Resolution. *Atmospheric Environment*, 167:403–415, 2017.

[19] IMO. Fourth IMO GHG Study 2020. Technical report, International Maritime Organization (IMO), London, UK, 2020.

[20] Jukka-Pekka Jalkanen, Lasse Johansson, and Jaakko Kukkonen. A Comprehensive Inventory of the Ship Traffic Exhaust Emissions in the Baltic Sea from 2006 to 2009. *AMBIO*, 43(3):311–324, 2014.

[21] Huan Liu, Mingliang Fu, Xinxin Jin, Yi Shang, Drew Shindell, Greg Faluvegi, Cary Shindell, and Kebin He. Health and Climate Impacts of Ocean-Going Vessels in East Asia. *Nature Climate Change*, 6(11):1037–1041, 2016.

[22] Wendela Schim van der Loeff, Javier Godar, and Vishnu Prakash. A Spatially Explicit Data-Driven Approach to Calculating Commodity-Specific Shipping Emissions Per Vessel. *Journal of Cleaner Production*, 205:895–908, 2018.

[23] Huan Liu, Zhi-Hang Meng, Zhao-Feng Lv, Xiao-Tong Wang, Fan-Yuan Deng, Yang Liu, Yan-Ni Zhang, Meng-Shuang Shi, Qiang Zhang, and Ke-Bin He. Emissions and health impacts from global shipping embodied in US–China bilateral trade. *Nature Sustainability*, 2(11):1027–1033, 2019.

[24] Anca Cristea, David Hummels, Laura Puzzello, and Misak Avetisyan. Trade and the Greenhouse Gas Emissions from International Freight Transport. *Journal of Environmental Economics and Management*, 65(1):153–173, 2013.

[25] Xiao-Tong Wang, Huan Liu, Zhao-Feng Lv, Fan-Yuan Deng, Hai-Lian Xu, Li-Juan Qi, Meng-Shuang Shi, Jun-Chao Zhao, Song-Xin Zheng, Han-Yang Man, and Ke-Bin He. Trade-linked shipping CO2 emissions. *Nature Climate Change*, 11(11):945–951, 2021.

[26] Sharat Ganapati, Woan Foong Wong, and Oren Ziv. Entrepot: Hubs, Scale, and Trade Costs. *American Economic Journal: Macroeconomics*, 16(4):239–278, 2024.

[27] US EPA. Health and Environmental Effects of Particulate Matter (PM), June 2024.

[28] Richard Klotz and Julia Berazneva. Local Standards, Behavioral Adjustments, and Welfare: Evaluating California's Ocean-Going Vessel Fuel Rule. *Journal of the Association of Environmental and Resource Economists*, 9(3):383–424, 2022.

[29] Janet Currie, John Voorheis, and Reed Walker. What Caused Racial Disparities in Particulate Exposure to Fall? New Evidence from the Clean Air Act and Satellite-Based Measures of Air Quality. *American Economic Review*, 113(1):71–97, 2023.

[30] Edgar G. Hertwich and Glen P. Peters. Carbon Footprint of Nations: A Global, Trade-Linked Analysis. *Environmental Science & Technology*, 43(16):6414–6420, August 2009.

[31] João F. D. Rodrigues, Daniel Moran, Richard Wood, and Paul Behrens. Uncertainty of Consumption-Based Carbon Accounts. *Environmental Science & Technology*, 52(13):7577–7586, July 2018. Publisher: American Chemical Society.

[32] Subsidiary Body for Scientific and Technological Advice, UNFCCC. Report of the Subsidiary Body for Scientific and Technological Advice on the Work of Its Fourth Session, Geneva, 16-18 December 1996. Technical report, UNFCCC, 1996.

[33] US EPA. Assessment of the Impacts of the Marpol Annex Vi Emission Control Regulations in the United States Portion of the North American Emission Control Area. Technical report, IMO Sub-Committee on Pollution Prevention and Response, 2023.

[34] US Department of State, Office of the Spokeperson. Green Shipping Corridors Framework, April 2022.

[35] John Keilman. America Is Back in the Factory Business. *Wall Street Journal*, April 2023.

[36] Pol Antras and Davin Chor. Global Value Chains. In *Handbook of International Economics*, volume 5. Elsevier, 5th edition, 2021.

[37] Wassily Leontief. Environmental Repercussions and the Economic Structure: An Input-Output Approach. *The Review of Economics and Statistics*, 52(3):262–271, 1970.

[38] Angel Aguiar, Maksym Chepeliev, Erwin Corong, and Dominique van der Mensbrugghe. The Global Trade Analysis Project (GTAP) Data Base: Version 11. *Journal of Global Economic Analysis*, 7(2), 2022.

[39] UNSD. UN Comtrade Database, 2024.

[40] Guillaume Gaulier and Soledad Zignago. BACI: International Trade Database at the Product-Level (the 1994-2007 Version). Technical report, 2010.

[41] Giulia Brancaccio, Myrto Kalouptsidi, and Theodore Papageorgiou. Geography, Transportation, and Endogenous Trade Costs. *Econometrica*, 88(2):657–691, 2020.

[42] Treb Allen and Costas Arkolakis. The Welfare Effects of Transportation Infrastructure Improvements. *The Review of Economic Studies*, 2022.

[43] Nicholas Z. Muller, Robert Mendelsohn, and William Nordhaus. Environmental Accounting for Pollution in the United States Economy. *American Economic Review*, 101(5):1649–1675, 2011.

[44] Stephen P. Holland, Erin T. Mansur, Nicholas Z. Muller, and Andrew J. Yates. Are There Environmental Benefits from Driving Electric Vehicles? The Importance of Local Factors. *American Economic Review*, 106(12):3700–3729, 2016.

[45] Andrew L. Goodkind, Christopher W. Tessum, Jay S. Coggins, Jason D. Hill, and Julian D. Marshall. Fine-Scale Damage Estimates of Particulate Matter Air Pollution Reveal Opportunities for Location-Specific Mitigation of Emissions. *Proceedings of the National Academy of Sciences*, 116(18):8775–8780, 2019. Publisher: Proceedings of the National Academy of Sciences.

[46] Christopher W. Tessum, Jason D. Hill, and Julian D. Marshall. InMAP: A Model for Air Pollution Interventions. *PLOS ONE*, 12(4):e0176131, 2017.

[47] Sumil K. Thakrar, Christopher W. Tessum, Joshua S. Apte, Srinidhi Balasubramanian, Dylan B. Millet, Spyros N. Pandis, Julian D. Marshall, and Jason D. Hill. Global, High-Resolution, Reduced-Complexity Air Quality Modeling for PM2.5 Using Inmap (intervention Model for Air Pollution). *PLOS ONE*, 17(5):e0268714, 2022.

[48] Global Burden of Disease Collaborative Network. Global Burden of Disease Study 2021 (GBD 2021). Technical report, Institute for Health Metrics and Evaluation (IHME), Seattle, United States, 2024.

[49] Daniel Krewski, Michael Jerrett, Richard T. Burnett, Renjun Ma, Edward Hughes, Yuanli Shi, Michelle C. Turner, C. Arden Pope, George Thurston, Eugenia E. Calle, Michael J. Thun, Bernie Beckerman, Pat DeLuca, Norm Finkelstein, Kaz Ito, D. K. Moore, K. Bruce Newbold, Tim Ramsay, Zev Ross, Hwashin Shin, and Barbara Tempalski. Extended Follow-up and Spatial Analysis of the American Cancer Society Study Linking Particulate Air Pollution and Mortality. Research Report 140, Health Effects Institute, Boston, Mass, 2009.

[50] Johanna Lepeule, Francine Laden, Douglas Dockery, and Joel Schwartz. Chronic Exposure to Fine Particles and Mortality: An Extended Follow-up of the Harvard Six Cities Study from 1974 to 2009. *Environmental Health Perspectives*, 120(7):965–970, 2012.

5 Tables and Figures

	Domestic	International	Total
Total Value (billion $)	123234	21458	144692
Merchandise	39586	17077	56663
Sea Value (billion $)	11313	8966	20279
Weight (billion tons)	16.3	9.5	25.7
Transport Services (trillion t-km)	26.8	91.1	117.9
Fuel (million tons)	67.3	166.1	233.4
Emissions (million tons)			
PM2.5	0.14	0.38	0.52
SOx	0.55	1.53	2.08
NOx	6.32	15.21	21.53
Mortality	93773	111376	205149
PM2.5	3453	3493	6945
SOx	15753	18108	33861
NOx	74567	89776	164343

Notes: Domestic versus international is determined by ultimate origin and destination countries of the goods traded. Merchandise row excludes services.

Table 1: Baseline Shipping Activity and Mortality

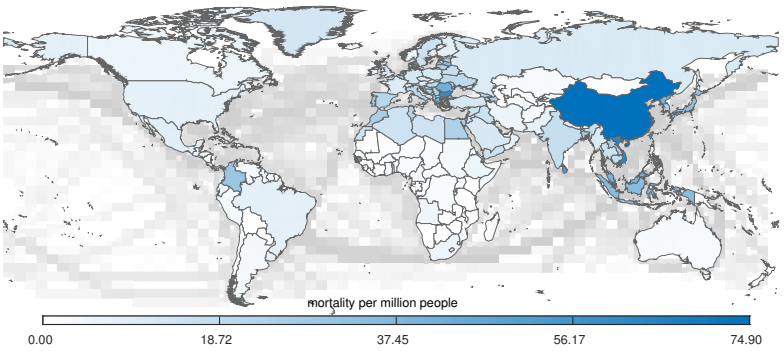

(a) Exposure

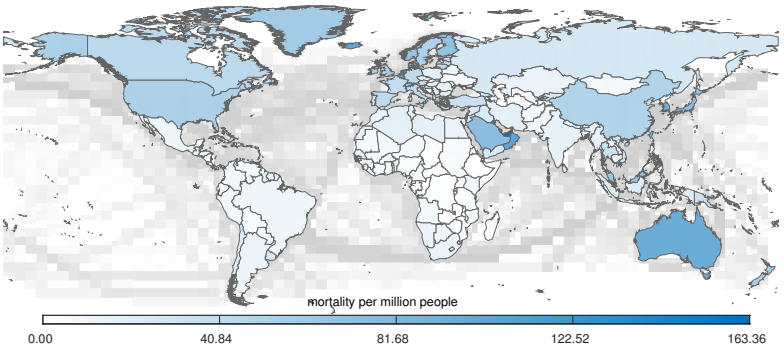

(b) Contribution

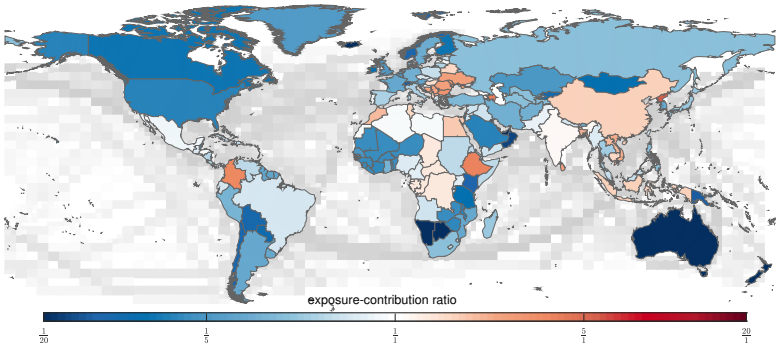

(c) Exposure-Contribution Ratio

Notes: gray shading over oceans depicts predicted fuel consumption by maritime vessels in each grid cell. Darker shades represent higher percentiles. In panels (a) and (b) the upper bound of color bar is 25% below maximum mortality.

Figure 1: Geographical Distribution of Exposure and Contributions

	Global	Low	Middle	High
Total	205149	54328	131340	19481
Own Consumption	74909	11472	59528	3909
Own Imports/Exports	35818	4988	28182	2648
Other Country Activity	94422	37868	43631	12924

Notes: Values in table are total mortality. Rows decompose a country's exposure to mortality resulting from own country consumption, from imports and exports to the country that are ultimately embodied in other countries' consumption, and from activities unrelated to that country. Calculations for each component of the decomposition are discussed in Methods.

Table 2: Decomposition of Contributions to Mortality

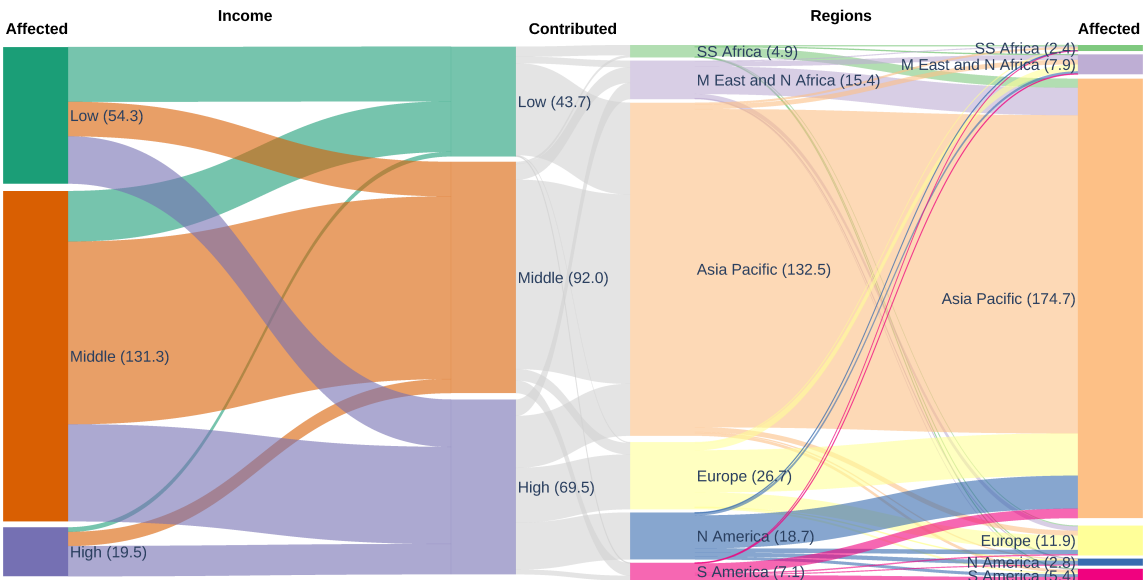

(a) Exposure and Contributions by Country Groups

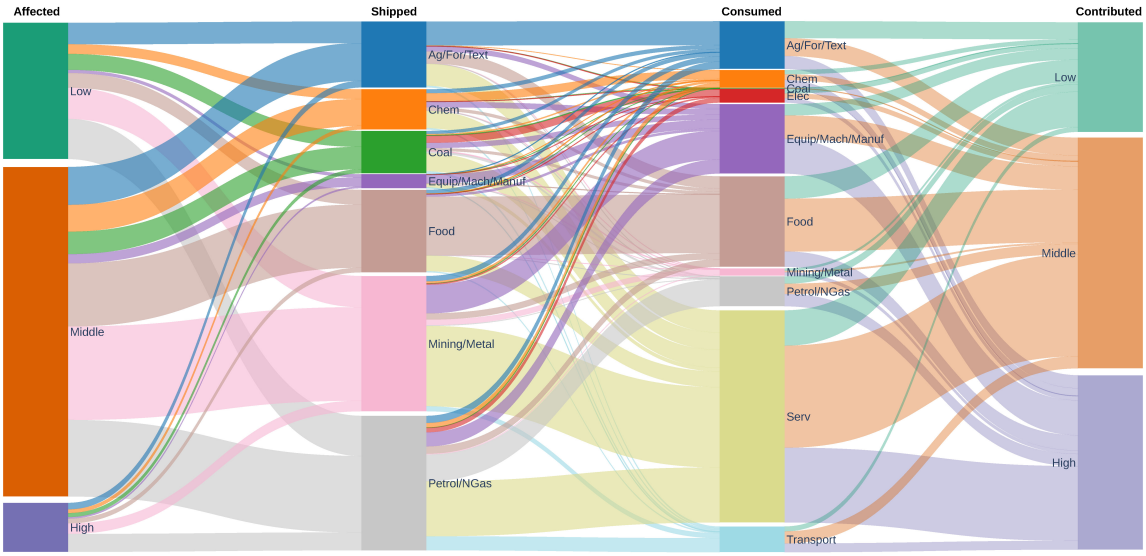

(b) Sectors Mediating Exposure and Contributions Across Income Groups

Panel (a): thousands of deaths by group reported in parentheses; income groups are based on World Bank Income Classifications as of 2017. Panel (b): expands left side of panel (a) to show contributions of goods consumed and shipped; aggregated to 10 sectors for clarity.

Figure 2: Shipping Mortality Exposure and Contributions

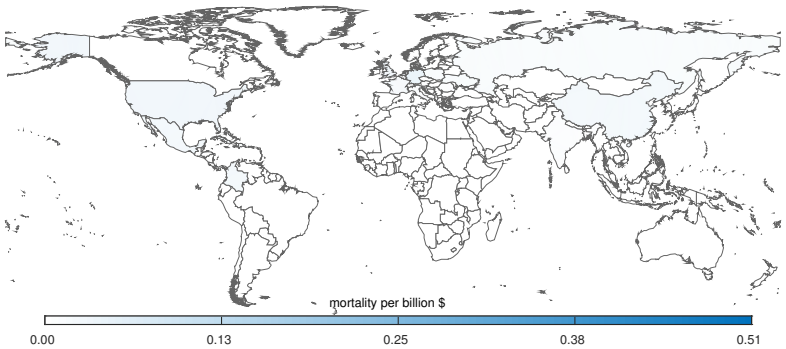

(a) Stage 0

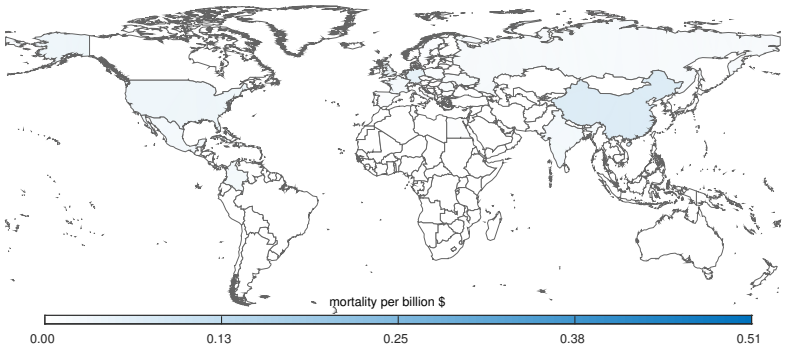

(b) Stage 1

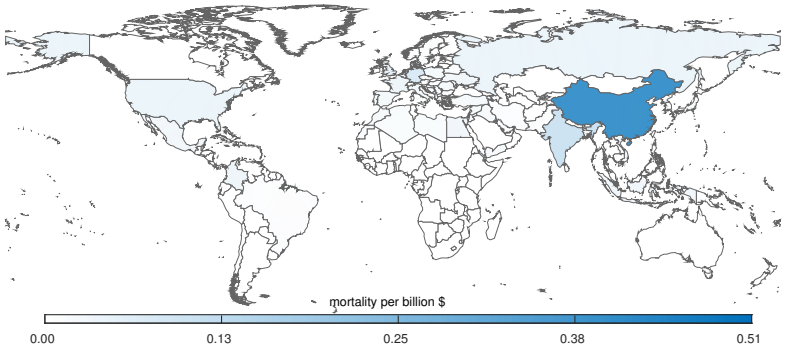

(c) Stage 4

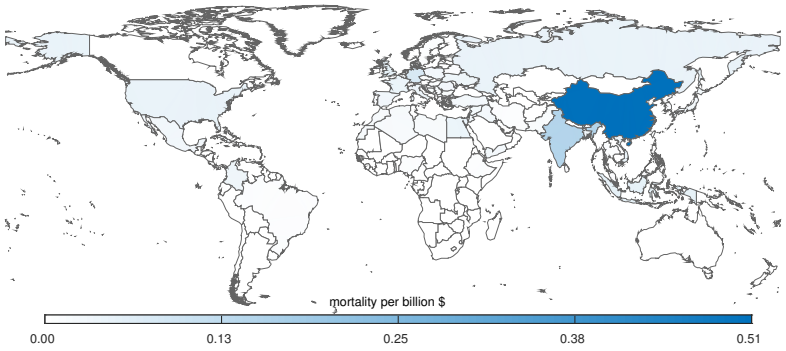

(d) Stage ∞

Notes: Shading depicts cumulative mortality through each production stage in each country. Upper bound of shading is 25% below maximum mortality.

Figure 3: Mortality Embodied in Germany-US Trade Over the Supply Chain

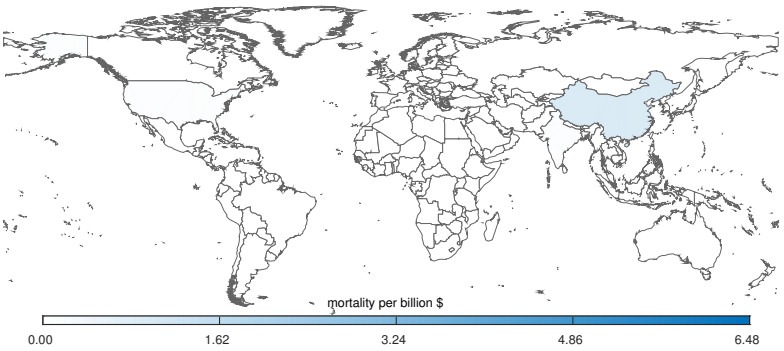

(a) Stage 0

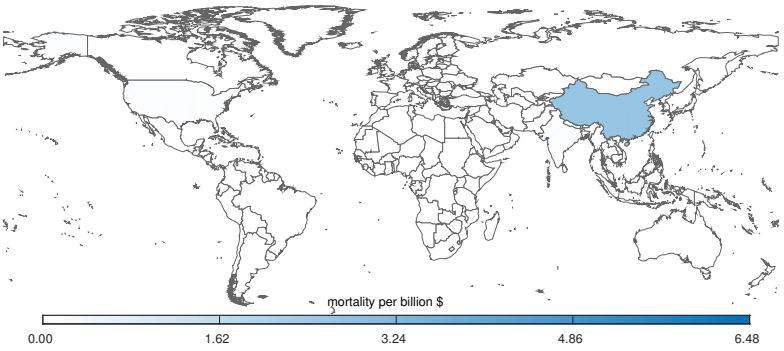

(b) Stage 1

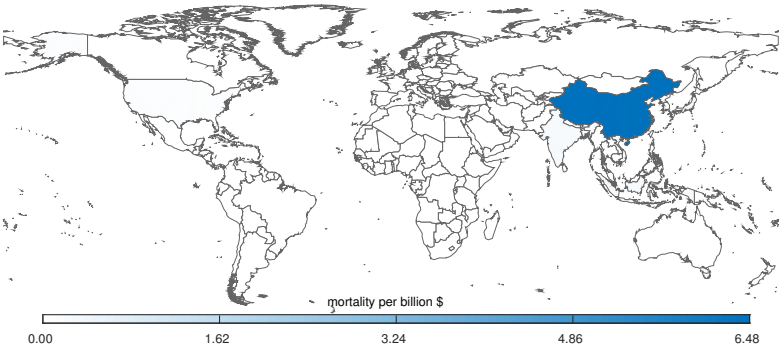

(c) Stage 4

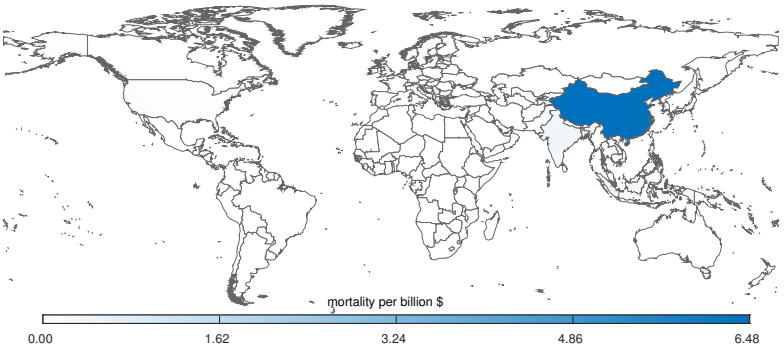

(d) Stage ∞

Notes: Shading depicts cumulative mortality through each production stage in each country. Upper bound of shading is 25% below maximum mortality.

Figure 4: Mortality Embodied in China-US Trade Over the Supply Chain

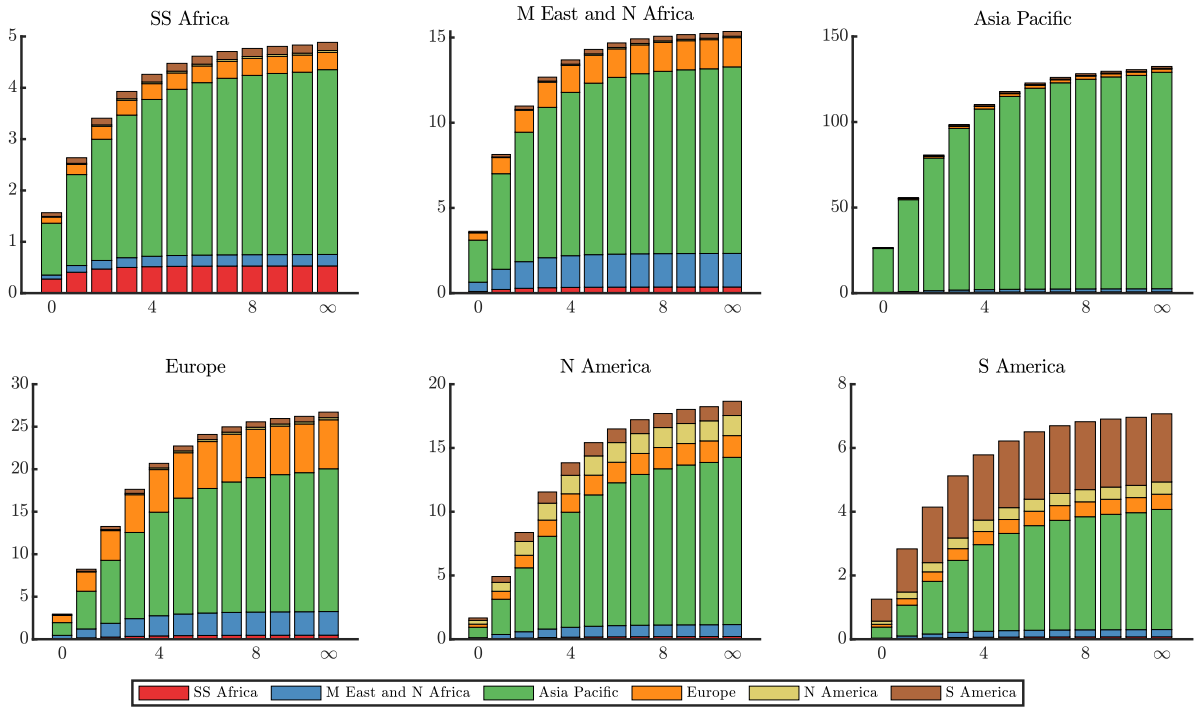

Notes: Bars reflect cumulative mortality (1000s of deaths) through each stage in the value chain. Stage 0 is the mortality associated with the shipping of final goods, stage 1 captures mortality associated with the shipping of final goods plus the shipping of inputs to those goods, etc. Stage ∞ is the mortality associated with all stages of production.

Figure 5: Regional Contributions to Mortality Over The Supply Chain

Stage	1	2	3	5	∞
mortality per capita	0.49	0.59	0.64	0.70	0.73
	(0.06)	(0.05)	(0.05)	(0.04)	(0.04)
	[0.31]	[0.48]	[0.58]	[0.68]	[0.74]
mortality/$	-0.51	-0.41	-0.36	-0.30	-0.27
	(0.06)	(0.05)	(0.05)	(0.04)	(0.04)
	[0.33]	[0.31]	[0.30]	[0.29]	[0.29]
$ sea/$	-0.22	-0.21	-0.20	-0.18	-0.17
	(0.06)	(0.05)	(0.04)	(0.04)	(0.03)
	[0.10]	[0.15]	[0.15]	[0.16]	[0.17]
kgkm/$ sea	-0.20	-0.11	-0.07	-0.05	-0.04
	(0.04)	(0.03)	(0.02)	(0.02)	(0.02)
	[0.20]	[0.10]	[0.07]	[0.04]	[0.03]
mort/kgkm	-0.09	-0.09	-0.09	-0.08	-0.07
	(0.04)	(0.03)	(0.03)	(0.03)	(0.02)
	[0.04]	[0.06]	[0.07]	[0.07]	[0.07]

Notes: Coefficients from linear regressions of the natural log of variables on the natural log of per capita income by country. Outcome variables are cumulative values up to and including the reported production production stage. Standard error of coefficient in parentheses and R^2 in square brackets. $N = 128$ for each regression since we drop a very minor region for which we lack port information. The final three rows decompose mortality per dollar as $\frac{mort}{\$} = \frac{\$sea}{\$} * \frac{kgkm}{\$sea} * \frac{mort}{kgkm}$ or the share of goods shipped by sea, shipping services per dollar shipped and mortality per unit of shipping.

Table 3: Regressions of Per Capita Contribution on Per Capita Income

	No ECAs	ECAs	IMO 2020
Total	375693	-9114	-170544
Low → Low	44757	-18	-22991
Low → Middle	28871	-54	-8786
Low → High	4432	-516	-2615
Middle → Low	26324	-50	-12607
Middle → Middle	126045	-173	-53391
Middle → High	13760	-1352	-8163
High → Low	37534	-150	-18688
High → Middle	62797	-586	-24196
High → High	31173	-6216	-19106

Notes: First column reports total emissions with no policies in place (fuel sulfur = 2.7%). ECAs column reports change in mortality when North and Baltic Sea and North American ECAs are in place with a fuel sulfur limit of 0.1%. IMO 2020 column reports additional change in mortality when fuel sulfur limit outside the ECAs is set to 0.5%.

Table 4: Mortality and Contributions Under Recent Policy Changes

		Low →			Middle →			High →		
	Total	Low	Middle	High	Low	Middle	High	Low	Middle	High
Central	205149	10.6	9.8	0.9	6.7	35.4	2.7	9.2	18.8	5.9
CR Sofiev (Low)	106118	11.3	9.6	0.8	7.1	34.7	2.6	9.8	18.6	5.6
CR Sofiev (High)	307991	10.4	9.8	0.9	6.6	35.6	2.8	9.0	18.9	6.0
CR Krewski	121251	14.3	8.3	1.0	8.3	30.0	3.2	12.0	16.4	6.6
CR LePeule	272655	14.3	8.3	1.0	8.3	30.0	3.2	12.0	16.4	6.6
Base Mort Low	179481	10.8	9.8	0.9	6.7	35.2	2.7	9.3	18.8	5.8
Base Mort Upper	230472	10.5	9.9	0.9	6.7	35.8	2.6	9.1	18.9	5.7
t/kgkm Cristea	233039	10.0	9.7	0.8	6.7	36.1	2.6	9.7	19.1	5.2
t/kgkm IMO	187408	10.1	9.5	0.8	6.9	33.9	2.6	10.7	19.8	5.6
Direct	174519	10.3	9.2	0.8	7.2	33.4	2.5	11.2	19.8	5.6

Notes: Sofiev [8], Krewski [49] and LePeule [50] rows alter the concentration-response function to other commonly used calibrations in the literature. The base mortality The t/kgkm rows use alternative global averages, by vessel type, for the fuel efficiency of vessels [24, 19]. Direct row assumes container vessels travel directly between origin-destination ports while using the global average fuel efficiency from [19]

Table 5: Mortality and Contributions Under Alternative Assumptions

Supplemental Material for "Global Value Chains Drive Disparities in the Health Consequences of Shipping"

April 2025

A Methods and Data

A.1 Attributing shipping damages to final consumption

We use input-output methods to calculate the shipping damages associated with final consumption. There are N countries and S sectors. Final demand is one of the S sectors. Define x_{ij}^{st} as the purchases of good s from country i used by sector t in country j, and $X = \{x_{ij}^{st}\}$. Final demand is Y_i^s, so total output is $X_i^s = \sum_{jt} x_{ij}^{st} + Y_i^s$ or in vector form X_{tot} The input-output matrix $A = X/diag(X_{tot})$ describes the dollars of good s from country i used by sector t in country j. Define $L = (I - A)^{-1} = A^0 + A^1 + A^2 + \ldots$ as the Leontief inverse matrix. The elements of L contain the additional units of each good that are needed (directly or indirectly) to produce an additional unit of each good. For example, L_{ij}^{st} is the additional amount of is that needs to be produced, for use at any stage of production, to support an additional unit of jt.

The marginal mortality in country k from moving a dollar of good is to jt (d_{ijk}^{st}) are:

$$d_{ijk}^{st} = s_{ij}^{s} * wv_{ij}^{s} * \sum_{ode} \theta_{ijod}^{s} * \pi_{ode}^{s} * m_{odek}^{s} \tag{2}$$

where s_{ij}^{s} is the share of each trade flow that travels by sea and wv_{ij}^{s} is the weight to value ratio for good s produced in country i. θ_{ijod}^{s} is the share of good s shipped from i to j that travels between ports o and d and π_{ode}^{s} is the probability that vessels carrying good s from port o to port d use edge e of the maritime network. Finally, m_{odek}^{s} is the mortality in country k associated with moving a ton of good s between port o and port d on edge e of

the maritime network. Note that the damage matrix does not vary with using sector t (i.e., $d^{st}_{ijk} = d^{s}_{ijk}$).

The total mortality from shipping, at any production stage, in each country that is eventually embodied in the vector (or matrix) of consumption Y is:

$$\tilde{D} = DLY$$

where N by $N * S$ matrix $D = \{\sum_{is} a^{st}_{ij} * d^{st}_{ijk}\}$ contains the mortality in each country k (rows) associated with the shipping of all inputs used to produce a unit of good jt.

A.2 Multi-region Input-output Matrix

To obtain the matrix X, we use the 2017 reference year from the GTAP 11B database. We aggregate this database to 20 sectors and 129 countries/regions (Tables A.5 and A.6). Consistent with the GTAP database, we assume that import shares (the share of good s used in country j from country i) are constant across industries and final consumers.

A.3 Marginal Mortality From Shipping

To obtain the marginal mortality from shipping, d^{st}_{ijk}, we first allocate each bilateral (country-to-country) trade flow to vessel types and port pairs, then to routes through a maritime network and ultimately to the quantity and location of emissions from shipping. We then calculate mortality associated with these emissions using a global source-receptor matrix that we constructed using a reduced complexity air quality model. This source-receptor matrix describes the increased mortality (in each country) associated with a ton of pollution emitted at each cell of a grid that covers the maritime network. The source-receptor approach – as opposed to simulating mortality associated with emissions on each link of the network – substantially reduces the computational burden of estimating mortality. We calculate marginal mortality for multiple pollutants ($PM_{2.5}$, SO_x and NO_x), though we drop this

subscript throughout for clarity.

The mortality associated with the movement of goods on each edge are the sum across all grid cells of the emissions released in each cell from a ton of good s moving on edge e multiplied by the mortality due to a ton of pollution emitted in that cell (md_{kg}):

$$m^s_{odek} = \sum_g (km_{eg} * f^s_{od} * ef^s_{ode}) * md_{kg} \tag{3}$$

where km_{eg} is the kilometers of edge e in grid cell g, f^s_{od} is a fuel consumption factor (kg fuel per km-kg of shipping services), and ef^s_{ode} is an emission factor (kg of emissions per kg fuel). The fuel consumption and emission factors vary by port pairs to account for geographical differences in the vessel fleet. The emissions factor is edge specific to account for ECAs, where vessels are required to use low sulfur fuels. The term in parenthesis is, therefore, the emissions released in cell g from a kg of good s moving on edge e, while md_{kg} is from the source-receptor matrix.

A.3.1 Mode Shares

Mode shares, s^s_{ij}, are derived from 2018 data from the UN Comtrade database [1]. Mode coverage in the Comtrade database is increasing over time. We use 2018 data to maximize coverage, while still avoiding the pandemic affected years starting in 2019. The Comtrade data reports values imported/exported between bilateral pairs of countries for 6-digit HS sectors. These flows are broken down by mode of transport for 82 countries (and 35-40% of value of trade reported in the database)[1]. We aggregate to our region and sector definitions and four modes (road, rail, air, sea, other) using FOB values when available and CIF values otherwise.

Given the structure of the Comtrade data, we can potentially calculate mode shares for the same bilateral flow using values reported by either the importer or the exporter. We use importer data when available – because importer data tends to be considered more reliable

[1]Mode shares are available for 40% of exports that report FOB values and 35% of imports that report CIF values.

– and only use the exporter (mirror) data when importer data is missing.

Our interest is the mode used by the primary leg of the journey. However, the mode reported in the Comtrade database represents the mode used when the goods left/entered the reporting country. If goods use foreign ports (e.g., leaving a country by road to get to a foreign port before traveling by sea to the final destination), which would be the case for landlocked countries, then the raw Comtrade data would greatly overstate the proportion of goods on land based modes. We address this issue by assigning any road and rail flows to sea if a land route between the trading partners is unlikely.[2] The key assumption here is that any goods leaving a country by land for a country for which a land route does not exist must travel by sea.

We fill in any missing international mode shares using the first available of the following mode shares (by sector): 1) those for the reverse bilateral pair (i.e., use the shares from country j to country i for the i to j flow); 2) subregion-to-subregion averages; 3) region-to-region averages; 5) subregion to any other subregion averages; 6) region to any other region averages. Regions and subregions are based on UN Statistical Division definitions. Intranational mode shares are constructed in two ways. First, for countries/regions in our data set that aggregate over multiple countries in the UNCTAD data we use the within country/region mode shares. Second, we use average mode shares between a country and its contiguous trading partners if those contiguous partners total at least 5% of total trade. Then we fill in missing values with the first available subregional, regional or global contiguous average mode shares.[3]

A.3.2 Weight-to-Value Ratios

Weight-to-value ratios are calculated at the country-pair by sector level from the 2018 BACI product-level trade database [2]. We winsorize the weight-to-value ratios at the 5th and 95th percentile, and replace any missing values with exporter-sector averages and then, if

[2]We assume that land routes are possible if both countries are either contiguous or in the same UN Statistical Division region, and if both countries are not islands.

[3]We also ensure that the sea share for domestic trade flows for landlocked countries is zero.

still missing, global averages at the sector level.

A.3.3 Sector-to-Vessel Type Categorization

We assign sectors to vessel types following prior literature [3]. Broadly speaking, raw materials are carried by bulkers (agriculture, coal, minerals) and tankers (oil, natural gas and refined oil products). Container ships are assumed to carry manufactured goods (machinery, equipment, manufactures) , while general cargo ships carry more unique products (chemicals, wood). These categorizations are consistent with [4].

A.3.4 Ports and Port Shares

There are no global databases of trade flows at the port-to-port level. Most researchers have inferred these port shares from observed vessel port calls or bill of ladings data [5, 6, 7], although modeling based approaches have also been used [8]. Following this earlier research, we obtain θ^s_{ijod} mainly from a global dataset of port calls for June 1st, 2014 to May 31, 2015 (purchased from Astra Paging). For non-containerized goods, we calculate the weight of goods moved between ports using the vessel calls data, and use these flows to calculate port shares. For the country pairs that we do not observe port flows we assign port shares proportionally to the total weight of goods arriving/departing at each port-pair ($\theta_{ijod} = \frac{tons_o}{tons_i} * \frac{tons_d}{tons_j}$, where $tons_i$ and $tons_j$ are the total weight of goods arriving/departing the country.) For containerized goods, we do not observe *od* flows in the port calls data (due to transhipment), so, as discussed above, we calculate port shares proportionally to the weight of goods arriving/departing each port pair.

Our sample of port calls contains all commercial cargo and tanker vessels operating world wide.[4] For each vessel, we observe the date/time and current draft when it enters and exits a port zone. Using IMO numbers we merge in vessel characteristics from a database obtained from Clarksons Research and Marine Traffic. These vessel characteristics include an aggregate vessel type grouping (container, tanker, bulker, general cargo), maximum draft and deadweight (DWT).

[4]We exclude ferries and smaller ro/ro vessels.

Since the draft data is likely more reliable when vessels are entering ports, we set a vessel's draft upon leaving a port to be equal to the draft reported at the following entrance.[5] This corrects unreasonably large changes in draft between an exit and the following entrance. We construct a data set of port calls by pairing consecutive entrances and exits.

Following [10] we estimate the total weight of goods carried by a vessel as $\frac{d-d_b}{d_m-d_b} * DWT$, where d is observed draft, d_b is ballast draft (draft when the vessel is not loaded), d_m is maximum draft and DWT is the vessels deadweight in tons. We estimate ballast draft as a fraction of maximum draft that varies by vessel type. Like [10] we use 0.55 for container ships. The fractions for other vessel types range from 0.44 to 0.52 and are derived from engineering relationships (e.g., [11]). The (net) weight of goods laden/unladen at a port is therefore the difference in total weight carried between the entrance and exit. We these values we can calculate the total weight of goods on vessels moving between two ports, and the total weight of goods laden and unladed at each port.

To calculate port shares for non-container vessels, we need to calculate the port-to-port flows of goods. A simple calculation of the weight laden/unladen at two consecutive ports is insufficient for this purpose because bulkers and tankers may lade at multiple ports, before then unlading at multiple ports. We use a simple vessel inventory model to calculate port-to-port flows of goods that account for this behavior. This model tracks the lading port of the goods on board the vessel. The goods unladen at any port are assumed to come proportionally from the goods currently on the vessel and after each unlading step the inventories are updated.

For example, suppose a vessel loads 20 tons of goods at port A and 80 tons of goods at port B, then unloads 50 tons at port C. The model would treat this as 10 tons moving from A to C and 40 tons moving from B to C. Suppose the vessel then picked up another 20 tons from port D, before unloading at port E. The additional flows would be 10 tons from A to

[5]The draft data reported in AIS data is entered by vessel operators. The draft entered upon an entrance is likely more reliable because reporting draft is much more important when entering a port, when this information needs to be communicated to port authorities and is crucial to prevent groundings. Similar adjustments have been made other studies that rely on AIS data [9].

E, 40 tons from B to E and 20 tons from D to E.

The ports included in our analysis are selected in the following way. Since this port calls dataset uses detailed port definitions (e.g., Long Beach and Los Angeles are accounted for separately), we group ports based on geographic proximity within countries using a clustering algorithm after removing very small ports (DBSCAN using haversine distance, ϵ=50km and minimum group size of 1). After clustering, we keep any port that accounts for at least 1% of national weight handled (laden or unladen) by vessel type. We also designate "major" ports in each country as the largest ports that cumulatively make up 90% of total national weight handled. When constructing port shares, we only consider major port pairs for international flows, but all ports are included when construction port pairs for intranational flows. Therefore the very smallest ports only move goods to the larger ports in the same country.

A number of countries do not have ports in the port calls data. For landlocked countries, we assign trade flows to the two closest ports to capital city of the land locked country (for each vessel type). For countries with important ports that are missing in the port calls data (which occurs for a few Central American countries), we include the largest port in each country based on total vessel calls in 2019 reported by the UN (`https://comtrade.un.org/data/monitor#AISPort`). To construct the size of each these port we multiply total vessel calls by the global average weight carried per vessel call by type. The final dataset contains 684 ports.

A.3.5 Edge Probabilities

The edge probabilities, π^s_{ode}, are the product of port-to-port probabilities π^s_{odmn} and route probabilities π^s_{mne}. The route probabilities, π_{mne}, allocate vessels moving between port m and port n to edges (e) of the shipping network. We determine π_{mne} by finding the minimum cost (distance) route between each port pair through the maritime network using Djikstra's algorithm. If edge e is on the route between m and n then $\pi_{mne} = 1$, otherwise this element is zero.

The shipping network is from Eurostat's SeaRoute program (`https://github.com/eurostat/searoute`), which is based on Oak Ridge National Lab's Global Shipping Lane Network with increased resolution around Europe based on AIS data. We updated this network in two ways. First, we added edges between each port in our analysis and the closest node in the maritime network. Second, we added edges to the network based on observed vessel trajectories if port-to-port routes based on the original network are substantially longer (300km) than the observed trajectories. We add edges in this way for the top 100 ports by tonnage. The observed vessel trajectories are described here: `https://towardsdatascience.com/creating-sea-routes-from-the-sea-of-ais-data-30bc68d8530e`.

The port-to-port probability, π^s_{odmn}, is the probability that a good ultimately moving from an origin port o to destination port d travels between any other pair of ports m and n. To broadly follow the structure of shipping markets, goods carried by tankers, bulk carriers and other cargo ships are assumed to move directly between origin and destination ports along the least cost route. For these vessels π^s_{odmn} equals 1 when $o = m$ and $d = n$, and is otherwise zero.

For container ships, we use the routing model from [12] to obtain values for π^s_{odmn} that captures indirect routing and transhipment. Container ships operate on a network that contains P ports. The ad-valorem costs of moving from port m to port n – which we refer to as link mn – is given by t_{mn}. Transportation costs are set to infinity for links that do not exist in the transportation network.

There are many combinations of port-to-port links that connect any origin and destination port. The total costs of moving goods on a particular set of links (a route) between two ports depends on the product of the link costs across all links used and an idiosyncratic route-level shock. The route-level shock introduces a dispersion in route choice that better reflects the data, particularly in the context of congestion [7].

Assuming that the route-level shock is distributed Fréchet with a shape parameter α,

then the transportation costs for moving goods through the network from port o to port d are:

$$\tau_{od} = (I - T^{-1})^{\circ(-\alpha)} \tag{4}$$

where $T = \{t_{mn}^{-\alpha}\}$, and $\circ$ refers to the Hadamard (element-wise) power. The port-to-port probabilities are:

$$\pi_{odmn} = \left(\frac{\tau_{om} t_{mn} \tau_{nd}}{\tau_{od}}\right)^{-\alpha}. \tag{5}$$

We calibrate link-level trade costs to match observed port-to-port flows derived from the port calls data using a procedure from [7]. This allows the calibrated model to reflect observed indirect shipping and transhipment.

We assume that link costs are $t_{mn}^{-\alpha} = \frac{1}{1+\exp(Z\beta)}$. Z contains factors that affect link-level shipping cost, like distance and traffic. α is set to 8 [7].

Given Z and β the predicted port-to-port probabilities are $\hat{\pi}_{odmn}(\beta, Z)$ and the predicted total tonnage of goods moving on each link in the transportation network is:

$$\hat{w}_{mn}(Y, \beta) = \sum_{od} \hat{\pi}_{odmn}(Y, \beta) w_{od} \tag{6}$$

where $w_{od} = \sum_{ijt} \sum_{s \in S_{cont}} X_{ij}^{st} * s_{ij}^{s} * wv_{ij}^{s} * \theta_{ijod}^{s}$ is the tonnage of containerized goods ultimately moving from port o to port d (S_{cont} is the set of sectors that are containerized). We then estimate β using generalized method of moments (GMM) to minimize the distance between the predicted and observed tonnage traveling on each link: $\hat{w}_{mn}(Y, \beta) - w_{mn}$. The moments are weighted by the inverse of observed link-level tonnage and exclude links between ports in the same countries. We exclude the domestic links because tonnage on these links will be underrepresented in areas where significant shares of coastal shipping occurs on vessels that are not in global vessel inventories, such as China [13]. Given an estimated vector of β we can obtain the full matrix of link-level costs, route-level costs, and port-to-port probabilities. It is important to note that our analysis does not rely on a causal interpretation of β. Rather

the goal is to find link-level costs that are as consistent with both observed trade flows and container ship patterns.

The selection criteria for the ports included in the container network are discussed above. We drop small links from the network – less than 2% of total origin or destination port tonnage – provided there are fewer then 10 total vessel trips observed on this route in the data. We consider specifications that include the logs of distance, origin, and destination traffic and link-level traffic. Traffic is measured as the total weight of goods carried by all the vessels that arrive/depart from each port or that are moving on a link. The GMM objective function has multiple local minima. To obtain a plausible global minimum we start the optimization routine from 250 random initial vectors, then take the minimum obtained across all initial vectors.

Results of our calibration procedure are reported in Table A.8. Column (1) reports model fit when distance is the only determinant of link-level transportation costs and the coefficient on distance is set to 1. The correlation between observed and model predicted link tonnage is 0.4, though the correlation using logged tonnage is somewhat higher. The calibrated versions fit much better. When link-level costs depend on distance and origin/destination tonnage model fit – as measured by root mean weighted squared error or the square root of the GMM objective function – improves dramatically. The correlation between observed and predicted tonnage increases to 0.585 (note that the reported correlations include links that are not matched in the calibration). Adding link-level tonnage improves model fit further, with the correlation between predicted and observed tonnage reaching 0.684 (0.77 when tonnage is logged). We also explore a specification that includes an indicator for backhaul links – when tonnage on a link is less than tonnage moving in the opposite direction on the same link. We use specification (3) for our main results because adding backhaul does little to improve model fit.

A.3.6 Fuel Consumption and Emission Factors

We derive fuel consumption and emission factors based on literature sources and the port calls data. The port calls data allows us to obtain factors that reflect the geographical differences in the vessel fleet.

We calculate average fuel consumption factors by bilateral port pairs (origin-destination) from the port calls data. For each trip – vessel moving between two ports – we calculate fuel consumption per ton-kilometer accounting for main and auxiliary engines based on:

$$\frac{f_{main}\left(\frac{s}{\bar{s}}\right)^2 + \frac{f_{aux}}{s}}{tons} \tag{7}$$

where f_{main} is fuel consumption per kilometer at design speed for main engines, f_{aux} is fuel consumption per hour for auxiliary engines, s is speed traveled, $\bar{s}$ is design speed of the vessel and $tons$ is weight carried by the vessel. The first term in the numerator is fuel consumption by main engines. The quadratic relationship between fuel consumption and speed derives from the propeller law and provides reasonable predictions of fuel consumption [14]. The quadratic relationship is also captured in the more complicated relationships often used in inventory studies [15].

We obtain f_{main} from our vessel characteristics database by dividing fuel consumption per hour at design speed by design speed. We scale the reported fuel consumption values to account for efficiency losses due to weather (15%) and hull fouling (9%) [15]. f_{aux} varies by vessel type and size and is from [15]. It is not possible to obtain accurate vessel speeds from the port calls data, so we assume there to be a constant ratio of observed to design speed by vessel type. We obtain these ratios from [15], but adjust for the fact that fuel consumption at the average speed will under predict average fuel consumption. We then average the vessel specific fuel consumption factors by bilateral pair. We fill missing values using the destination-origin pair and then the first available average at the port-to-country, port, country-to-country, country or region level.

Emission factors for primary $PM_{2.5}$ and SO_2 follow IMO greenhouse gas inventories [16, 15] and depend on the sulfur content of the fuel being used. We assume fuel sulfur is 2.7% if no policies are in place, and that the limits imposed by IMO 2020 (0.5%) and ECAs (0.1%) are binding when these policies are considered. For SO_2, the emission factor accounts for the fraction of fuel sulfur that is converted to SO_x and the molecular weight of SO_2: $ef(SO_2) = sulfur/100 * 0.9754 * 2$ where $sulfur$ is the percent of sulfur in fuel by weight (0 to 100 scale). The IMO inventory reports relationships between fuel sulfur and $PM_{2.5}$ emissions (g/kWh) for residual and distillate fuels. These relationships – after converting to g/g fuel – are:

$$
\begin{aligned}
ef_r &= (1.35 + sfc * 7 * 0.02247 * (sulfur/100 - 0.0246)) * 0.92/sfc \\
ef_d &= (0.23 + sfc * 7 * 0.02247 * (sulfur/100 - 0.0024)) * 0.92/sfc
\end{aligned} \tag{8}
$$

where sfc is the specific fuel consumption factors (g/kWh) and the subscripts r and d designate residual and distillate fuel respectively. We use the residual emission factor for sulfur levels above 1%, the residual emission factor for sulfur levels below 0.25%, and linear combination of the two fuels that achieves the appropriate sulfur level for the intermediate range.

NOx emissions are regulated by IMO standards, which are tiered by age [17]. We construct ef^s_{ode} for NOx as the average of the tiered emission standards weighted by the tons carried by vessels of each tier between port o and d, which we obtain from the port calls database. The IMO standards set emissions limits per kilowatthour (Table A.7), which we convert to emissions per unit fuel by dividing by specific fuel consumption factors (g/kWh). The specific fuel consumption factors are from [15] and assume that vessels vessels operate at approximately 80% load and use heavy fuel oil. We do not consider Tier III standards, which only applies in North America ECA in 2016 and in North and Baltic ECAs in 2021, in our main analysis because our port calls data is from prior to 2016 and because there is

some concern related to the effectiveness of these standards [18].

A.3.7 Source-Receptor Matrix

We use a global version of InMap to construct our source-receptor matrix [19, 20]. InMap uses a variable size computational grid that gets smaller in highly populated areas. A limitation of the current version of InMap is that pollution is not tracked across the poles or antimeridian. The resolution of our source-receptor matrix broadly matches the computational grid used in [20]. Grid cells in the open ocean are 5° by 4°, while cells that intersect land are 2.5° by 2°. We drop grid cells that do not intersect with an edge in the maritime network. There are 3,058 cells in the source-receptor grid.

We use InMap to simulate the change in ambient particulate matter (in each cell of InMap's computational grid) associated with the a one ton emission in each cell in the source-receptor matrix (and for each pollutant). To limit the computational burden of this exercise, we limit the NOx source-receptor matrix to the 2,375 cells with the highest contributions to mortality per ton $PM_{2.5}$. This set of cells account for well over 99% of mortality related to $PM_{2.5}$ emissions. This restriction effectively limits coverage of the NOx grid in open oceans that are distant from population centers and should have little meaningful impact on our results.

For each cell in InMap's grid, we then estimate the change in mortality due to the change in ambient particulate matter. We sum over the InMap grid cells by country to get country level estimates of mortality per ton of emission. Mortality is related to a change in pollution concentration according to: $mort = AF * base * pop$ where AF is the attributable fraction, *base* is baseline mortality rates and *pop* is population. Attributable fraction related to relative risk according to: $AF = (RR - 1)/RR = 1 - RR^{-1}$. We use a log-linear relative risk function – following [21, 22, 23, 24] – to obtain:

$$mort = (\exp(\beta * \Delta_{PM}) - 1) * base * pop \tag{9}$$

where β is a parameter from the literature and Δ_{PM} is the change in ambient particulate matter simulated by InMap. Note that this specification is relevant for small changes in concentrations. There are other functional form options for relative risk, including the integrated exposure-response (IER) function. We use the log-linear specification for computational simplicity, to be consistent with other studies of the health burden of shipping, concerns that the IER function will underpredict mortality in more polluted areas [25], and because the log-linear specification is consistent with recently developed models when evaluating a marginal changes in concentrations [26].

Our population data is the 2020 projected population from [27]. We obtain baseline mortality rates, averaged over 2015-2019, at the country level from [28]. The upper and lower estimates from this source are used in our sensitivity analysis. We generate results using a number of assumptions for β. Our main results follow [22] who use $\beta = 0.023111(0.013103, 0.033647)$ for cardiovascular mortality and $\beta = 0.031481(0.006766, 0.055962)$ for lung cancer related mortality. We also generate results with the commonly used parameter estimates from Krewski et al. (2009) [29] and LePeule et al. (2012) [30], which imply a 6% or 14% increase in all cause mortality for a 10 microgram per cubic meter increase in particulate (β is 0.0058 or 0.0131).

B Validation of Top-Down Accounting

Table 1 presents baseline estimates for maritime shipping, broken down both by domestic and international trade flows. Our top-down accounting of shipping activity, fuel use and emissions are in general accordance with comparable global statistics and, in the case of emissions and mortality, inventory studies of the local pollution externality from shipping.

The GTAP data reports $21 trillion in international trade and $17 trillion in international merchandise trade. This is comparable to the total value of merchandise trade (exports) in 2017 of $17.2 trillion reported by UNCTAD [31]. The total value of international maritime trade is $9 trillion (or 53% of total), which is roughly consistent with estimates that put the share of maritime trade by value to be between 50%-70% [8, 32, 33]. The IATA also reports that about 35% of international trade by value is by air, which implies a sea share in this range [34]. However, our approach underestimates the weight and shipping services associated with international trade reported by UNCTAD (10.7 billion tons loaded and 107.4 trillion t-km in 2017), though we estimate a very similar value for kilometers traveled per ton of goods shipped.

Breaking weight traded down by vessel type, [31] report weight of trade by product type: 30% is oil and gas, 30% is other bulk (iron ore, coal, grain, etc) and 40% is other dry cargo. This breakdown broadly fits with our vessel designations if we combine our container and general cargo to represent other dry cargo, though we somewhat under represent other dry cargo (Table A.1).

Since fuel consumption by maritime transport and, especially, emissions are not directly observable on the global scale, the most direct comparisons of our estimates are to inventory studies of the maritime transport sector. Our fuel consumption and emissions values are generally in line with these studies, considering our somewhat lower estimate of weight and transportation services. We estimate fuel consumption of 166 and 67 million tons for international and domestic shipping respectively. [15] reports similar numbers based on

bunker fuel sales (221.47 and 48.98 million tons) and an AIS inventory (225.34 and 30 million tons) methodologies. Total fuel consumption estimated by [22] using AIS inventory methods is very similar. Our breakdown of domestic versus international fuel use are not directly comparable to these studies because our definition is based on the trade flow as opposed to the vessel type and ports used. Perhaps more informatively, our average fuel consumption per unit of transportation service (2.0 tons per million t-km) is quite similar to both of these studies. Compared to [15], our estimate is nearly identical to the global average reported for 2015, but is somewhat higher than reported global average in 2018. Given the relatively close accordance with fuel consumption, our predicted emissions are also consistent with [15] and [22], when IMO 2020 and ECAs are accounted for.

Despite substantial differences in modeling, our accounting provides estimates of mortality that are consistent with other recent studies of total air pollution related mortality of shipping. Soviev et al. [22] use a shipping inventory model and a high complexity atmospheric model to estimate shipping mortality to be 403 (212-595) thousand when ECAs and EU and Chinese sulfur directives are in place but IMO 2020 is not. Our estimates using the source-receptor matrix compare favorably – 366 thousand deaths – when the ECAs are in place (Table 4).

C Appendix Tables and Figures

	Bulker	Container	Gen. Cargo	Tanker	Total
Total Value (billion $)	6913	43742	756	5251	144692
Merchandise	6913	43742	756	5251	56663
Sea Value (billion $)	2065	14928	234	3053	20279
Weight (billion tons)	9.0	8.0	0.3	8.5	25.7
Transport Services (trillion t-km)	50.7	31.2	1.3	34.7	117.9
Fuel (million tons)	80.3	78.1	7.2	67.9	233.4
Emissions (million tons)					
PM2.5	0.18	0.18	0.02	0.14	0.52
SOx	0.74	0.73	0.06	0.55	2.08
NOx	7.26	7.27	0.67	6.33	21.53
Mortality	54461	91579	5511	53598	205149
PM2.5	1655	3298	178	1814	6945
SOx	8583	15343	886	9049	33861
NOx	44223	72938	4446	42735	164343

Notes: Merchandise row excludes services.

Table A.1: Baseline Shipping Activity and Mortality

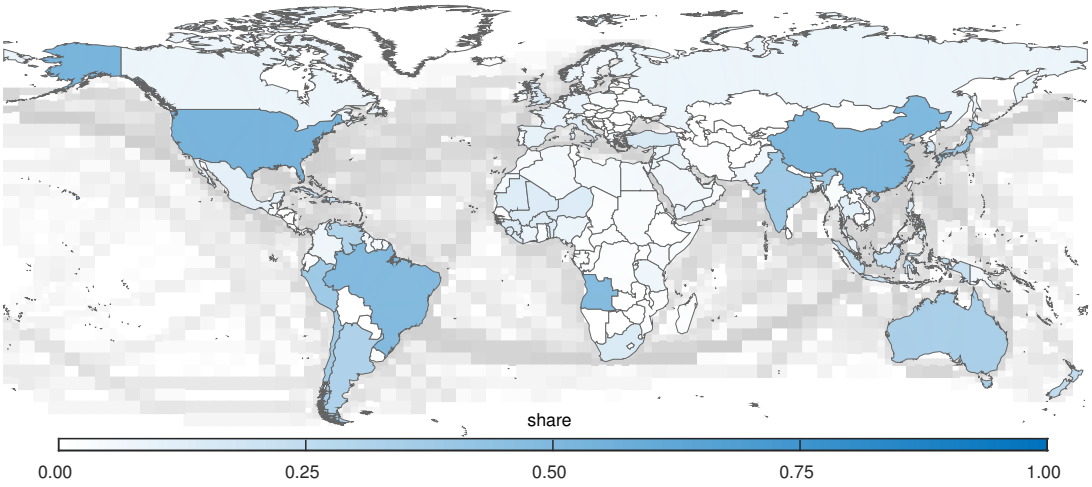

(a) Own Consumption

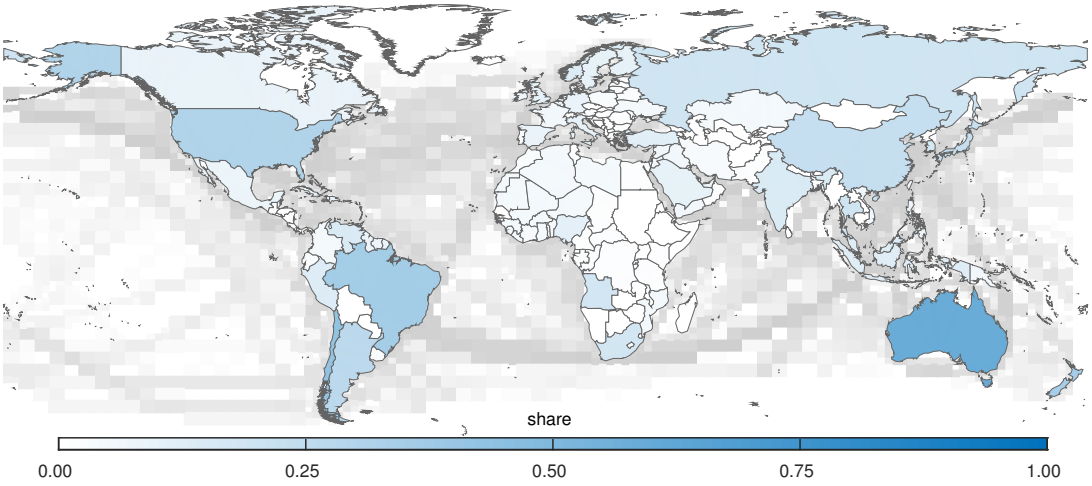

(b) Imports and Exports Embodied in Other's Consumption

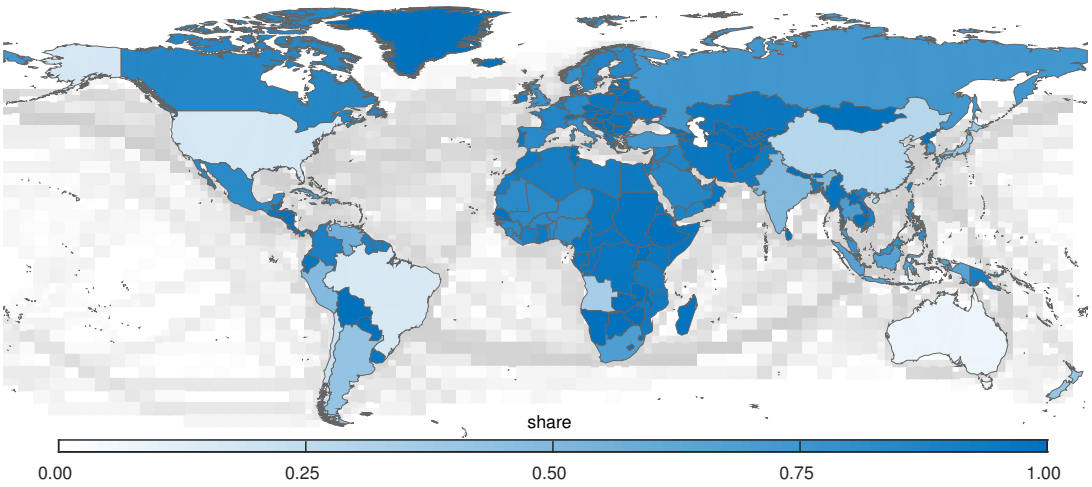

(c) Other Countries' Activities

Figure A.1: Decomposition of Exposure

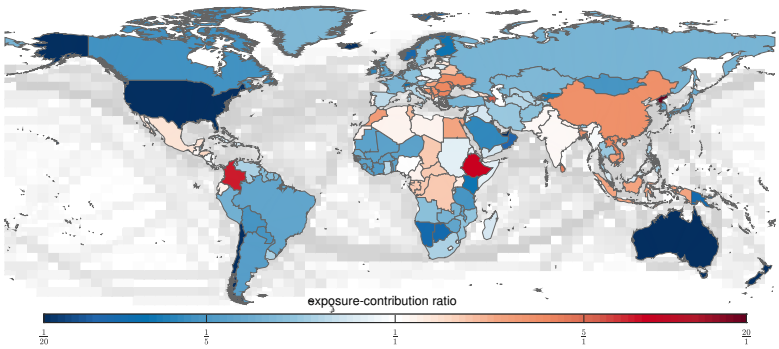

Notes: gray shading represents predicted fuel consumption in each grid cell. Darker shades represent higher percentiles.

Figure A.2: Other Country Exposure-Contribution Ratio

	Consumption	Imports	Exports
SS Africa → SS Africa	530	717	606
SS Africa → M East and N Africa	223	167	173
SS Africa → Asia Pacific	3600	3700	2448
SS Africa → Europe	336	298	258
SS Africa → N America	37	43	29
SS Africa → S America	159	185	152
M East and N Africa → SS Africa	360	449	359
M East and N Africa → M East and N Africa	1971	2425	2132
M East and N Africa → Asia Pacific	10945	15841	8644
M East and N Africa → Europe	1715	1720	1715
M East and N Africa → N America	86	82	59
M East and N Africa → S America	277	162	222
Asia Pacific → SS Africa	762	404	798
Asia Pacific → M East and N Africa	1809	1298	1708
Asia Pacific → Asia Pacific	126498	129662	148043
Asia Pacific → Europe	1903	1448	1474
Asia Pacific → N America	429	150	359
Asia Pacific → S America	1064	348	974
Europe → SS Africa	475	402	460
Europe → M East and N Africa	2779	2935	3057
Europe → Asia Pacific	16796	11590	10127
Europe → Europe	5762	6181	6713
Europe → N America	252	125	166
Europe → S America	652	360	536
N America → SS Africa	210	102	145
N America → M East and N Africa	938	670	770
N America → Asia Pacific	13116	4988	4225
N America → Europe	1704	1474	1405
N America → N America	1576	2023	1773
N America → S America	1116	1495	1051
S America → SS Africa	75	338	45
S America → M East and N Africa	227	452	107
S America → Asia Pacific	3769	8944	1238
S America → Europe	477	776	333
S America → N America	385	341	377
S America → S America	2137	2855	2469

Notes: First column allocates contributions based on on consumption using input-output methods. Remaining columns allocate contributions based on imports (second column) and exports (third column).

Table A.2: Alternative Attribution Options

	IMO 2020	Med	China	India
Total	205149	-2441	-11832	-3234
Low → Low	21766	-173	-36	-2254
Low → Middle	20085	-114	-770	-49
Low → High	1817	-95	-38	-2
Middle → Low	13716	-266	-218	-285
Middle → Middle	72654	-232	-8026	-4
Middle → High	5597	-173	-403	-0
High → Low	18846	-518	-86	-630
High → Middle	38601	-416	-2146	-10
High → High	12067	-454	-111	-0

Notes: First column report results with IMO 2020 and current ECAs in place. Remaining columns report changes in mortality with ECAs established in the Mediterranean Sea, and the Exclusive Economic Zones of China and India.

Table A.3: Mortality and Contributions Under Alternative ECAs

	Baseline	Effic Global	Reshore USA	Reshore China
Total	205149	-15220	-3535	-3471
Low → Low	21766	-1643	-14	-85
Low → Middle	20085	-1383	-29	-113
Low → High	1817	-138	-5	-21
Middle → Low	13716	-1055	-61	-1117
Middle → Middle	72654	-4036	-115	-1097
Middle → High	5597	-416	-21	-287
High → Low	18846	-1981	-885	-315
High → Middle	38601	-3353	-2090	-357
High → High	12067	-1214	-315	-79

Notes: First column reports results with IMO 2020 and current ECAs in place. Column (2) reports mortality with energy inputs per dollar of output reduced by 25% for all production sectors globally. Columns (3) and (4) reports results when share foreign goods in both production and consumption is reduced by 25% and the share of domestic goods are scaled accordingly in US and China respectively.

Table A.4: Mortality and Contributions Under Alternative Scenarios

	GTAP Sectors
Agr	pdr; wht; gro; v_f; osd; c_b; pfb; ocr; ctl; oap; rmk; wol; frs; fsh
Chem	chm; bph; rpp
Coal	coa
Elec	ely
Equip	mvh; otn
Food	cmt; omt; vol; mil; pcr; sgr; ofd; b_t
Mach	ome
Mach_Ele	ele; eeq
Manuf	omf
Metal	i_s; nfm; fmp
Min	nmm
Mine	oxt
NGas	gas; gdt
Oil	oil
Other	wtr; cns; trd; afs; cmn; ofi; ins; rsa; ros; osg; edu; hht; dwe
P_C	p_c
Paper	ppp
Textile	tex; wap; lea
Transport	otp; wtp; atp; whs; obs
Wood	lum

Table A.5: Sector Aggregation

ALB-alb **ARE**-are **ARG**-arg **ARM**-arm **AUS**-aus **AUT**-aut **AZE**-aze **BEL**-bel **BGD**-bgd **BGR**-bgr **BHR**-bhr **BLR**-blr **BOL**-bol **BRA**-bra **BWA**-bwa **CAN**-can **CHE**-che **CHL**-chl **CHN**-chn **CIV**-civ **CMR**-cmr **COL**-col **CRI**-cri **CYP**-cyp **CZE**-cze **DEU**-deu **DNK**-dnk **ECU**-ecu **EGY**-egy **ESP**-esp **EST**-est **ETH**-eth **FIN**-fin **FRA**-fra **GBR**-gbr **GEO**-geo **GHA**-gha **GRC**-grc **GTM**-gtm **HKG**-hkg **HND**-hnd **HRV**-hrv **HUN**-hun **IDN**-idn **IND**-ind **IRL**-irl **IRN**-irn **ISR**-isr **ITA**-ita **JPN**-jpn **KAZ**-kaz **KEN**-ken **KGZ**-kgz **KHM**-khm **KOR**-kor **KWT**-kwt **LAO**-lao **LKA**-lka **LTU**-ltu **LUX**-lux **LVA**-lva **MAR**-mar **MDG**-mdg **MEX**-mex **MLT**-mlt **MNG**-mng **MOZ**-moz **MUS**-mus **MWI**-mwi **MYS**-mys **NAM**-nam **NGA**-nga **NIC**-nic **NLD**-nld **NOR**-nor **NPL**-npl **NZL**-nzl **OMN**-omn **PAK**-pak **PAN**-pan **PER**-per **PHL**-phl **POL**-pol **PRT**-prt **PRY**-pry **QAT**-qat **ROU**-rou **RUS**-rus **SAU**-sau **SEN**-sen **SGP**-sgp **SLV**-slv **SVK**-svk **SVN**-svn **SWE**-swe **THA**-tha **TUN**-tun **TUR**-tur **TWN**-twn **TZA**-tza **UGA**-uga **UKR**-ukr **URY**-ury **USA**-usa **VEN**-ven **VNM**-vnm **XAC**-xac **XCA**-xca **XCAR**-dom; hti; jam; pri; tto; xcb **XCF**-caf; tcd; cog; cod; gnq; gab **XEA**-xea **XEAF**-com; rwa; sdn; xec **XEE**-xee **XEF**-xef **XER**-srb; xer **XNA**-xna **XNF**-dza; xnf **XOC**-xoc **XSA**-afg; xsa **XSC**-swz; xsc **XSEAS**-brn; xse **XSM**-xsm **XSU**-tjk; uzb; xsu **XTW**-xtw **XWAF**-ben; bfa; gin; mli; ner; tgo; xwf **XWAS**-irq; jor; lbn; pse; syr; xws **ZAF**-zaf **ZMB**-zmb **ZWE**-zwe

Table A.6: Country Aggregation

	Age	gNOx/kWh	gNOx/g Fuel
Tier 0	Before 2000	18.1	$18.1/185 = 0.097838$
Tier I	After 2000	17	$17/175 = 0.097143$
Tier II	After 2011	14.4	$14.4/175 = 0.082286$
Tier III	After 2016	3.4	$3.4/175 = 0.019429$

Notes: gNOx/kWh is from [17]. The majority of vessels in our analysis use slow-speed engines – RPM lower than 130 – so we use the highest possible NOx rating in each tier.

Table A.7: NOx Emissions Factors

	(1)	(2)	(3)	(4)
cons	-	13.468	-4.421	-4.119
km	1.000	0.564	0.634	0.608
tons_o	-	-3.626	-0.266	-0.711
tons_d	-	1.200	2.170	2.604
tons_od	-	-	-1.810	-1.822
backhaul	-	-	-	-0.196
RMWSE * 1000	3.215	1.564	0.981	0.971
Correlation	0.402	0.585	0.684	0.683
Correlation (logs)	0.567	0.580	0.773	0.764

Notes: Column (1) reports model fit when coefficient on distance is set to 1. Remaining columns report estimation results with various specifications of link-level trade costs. km - is link distance by sea; tons_o, tons_d , tons_od are the weight of goods leaving the origin port, arriving at the destination port, and traveling on the link respectively. backhaul is an indicator for when tonnage on a link is less than tonnage moving in the opposite direction on the same link. All continuous variables are logged.

Table A.8: Routing Parameter Estimates

References

[1] UNSD. UN Comtrade Database, 2024.

[2] Guillaume Gaulier and Soledad Zignago. BACI: International Trade Database at the Product-Level (the 1994-2007 Version). Technical report, 2010.

[3] Anca Cristea, David Hummels, Laura Puzzello, and Misak Avetisyan. Trade and the Greenhouse Gas Emissions from International Freight Transport. *Journal of Environmental Economics and Management*, 65(1):153–173, 2013.

[4] Xiao-Tong Wang, Huan Liu, Zhao-Feng Lv, Fan-Yuan Deng, Hai-Lian Xu, Li-Juan Qi, Meng-Shuang Shi, Jun-Chao Zhao, Song-Xin Zheng, Han-Yang Man, and Ke-Bin He. Trade-linked shipping CO2 emissions. *Nature Climate Change*, 11(11):945–951, 2021.

[5] Huan Liu, Zhi-Hang Meng, Zhao-Feng Lv, Xiao-Tong Wang, Fan-Yuan Deng, Yang Liu, Yan-Ni Zhang, Meng-Shuang Shi, Qiang Zhang, and Ke-Bin He. Emissions and health impacts from global shipping embodied in US–China bilateral trade. *Nature Sustainability*, 2(11):1027–1033, 2019.

[6] Giulia Brancaccio, Myrto Kalouptsidi, and Theodore Papageorgiou. Geography, Transportation, and Endogenous Trade Costs. *Econometrica*, 88(2):657–691, 2020.

[7] Sharat Ganapati, Woan Foong Wong, and Oren Ziv. Entrepot: Hubs, Scale, and Trade Costs. *American Economic Journal: Macroeconomics*, 16(4):239–278, 2024.

[8] J. Verschuur, E. E. Koks, and J. W. Hall. Ports' criticality in international trade and global supply-chains. *Nature Communications*, 13(1):4351, 2022.

[9] Serkan Arslanalp, Robin Koepke, and Jasper Verschuur. Tracking Trade from Space: An Application to Pacific Island Countries. Technical Report WP/21/225, International Monetary Fund, 2021.

[10] Inga Heiland, Andreas Moxnes, Karen Helene Ulltveit-Moe, and Yuan Zi. Trade From Space: Shipping Networks and The Global Implications of Local Shocks. 2022.

[11] ShibataFenderTeam. Design Manual. Technical report, 2021.

[12] Treb Allen and Costas Arkolakis. The Welfare Effects of Transportation Infrastructure Improvements. *The Review of Economic Studies*, 2022.

[13] Xiaoli Mao and Zhihang Meng. Decarbonizing China's Coastal Shipping: The Role of Fuel Efficiency and Low-Carbon Fuels. Working Paper 2022-20, International Council on Clean Transportation, 2022.

[14] J.-P. Jalkanen, L. Johansson, J. Kukkonen, A. Brink, J. Kalli, and T. Stipa. Extension of an Assessment Model of Ship Traffic Exhaust Emissions for Particulate Matter and Carbon Monoxide. *Atmospheric Chemistry and Physics*, 12(5):2641–2659, 2012.

[15] IMO. Fourth IMO GHG Study 2020. Technical report, International Maritime Organization (IMO), London, UK, 2020.

[16] IMO. Third IMO GHG Study 2014. Technical report, International Maritime Organization (IMO), London, UK, 2015.

[17] IMO. Nitrogen Oxides (NOx) – Regulation 13, 2019.

[18] US EPA. Assessment of the Impacts of the Marpol Annex Vi Emission Control Regulations in the United States Portion of the North American Emission Control Area. Technical report, IMO Sub-Committee on Pollution Prevention and Response, 2023.

[19] Christopher W. Tessum, Jason D. Hill, and Julian D. Marshall. InMAP: A Model for Air Pollution Interventions. *PLOS ONE*, 12(4):e0176131, 2017.

[20] Sumil K. Thakrar, Christopher W. Tessum, Joshua S. Apte, Srinidhi Balasubramanian, Dylan B. Millet, Spyros N. Pandis, Julian D. Marshall, and Jason D. Hill. Global, High-Resolution, Reduced-Complexity Air Quality Modeling for PM2.5 Using Inmap (intervention Model for Air Pollution). *PLOS ONE*, 17(5):e0268714, 2022.

[21] Huan Liu, Mingliang Fu, Xinxin Jin, Yi Shang, Drew Shindell, Greg Faluvegi, Cary Shindell, and Kebin He. Health and Climate Impacts of Ocean-Going Vessels in East Asia. *Nature Climate Change*, 6(11):1037–1041, 2016.

[22] Mikhail Sofiev, James J. Winebrake, Lasse Johansson, Edward W. Carr, Marje Prank, Joana Soares, Julius Vira, et al. Cleaner Fuels for Ships Provide Public Health Benefits with Climate Tradeoffs. *Nature Communications*, 9(1):1–12, 2018.

[23] Christopher W. Tessum, Joshua S. Apte, Andrew L. Goodkind, Nicholas Z. Muller, Kimberley A. Mullins, David A. Paolella, Stephen Polasky, Nathaniel P. Springer, Sumil K. Thakrar, Julian D. Marshall, and Jason D. Hill. Inequity in Consumption of Goods and Services Adds to Racial–Ethnic Disparities in Air Pollution Exposure. *Proceedings of the National Academy of Sciences*, 116(13):6001–6006, 2019.

[24] Andrew L. Goodkind, Christopher W. Tessum, Jay S. Coggins, Jason D. Hill, and Julian D. Marshall. Fine-Scale Damage Estimates of Particulate Matter Air Pollution Reveal Opportunities for Location-Specific Mitigation of Emissions. *Proceedings of the National Academy of Sciences*, 116(18):8775–8780, 2019. Publisher: Proceedings of the National Academy of Sciences.

[25] Peng Yin, Michael Brauer, Aaron Cohen, Richard T. Burnett, Jiangmei Liu, Yunning Liu, Ruiming Liang, Weihua Wang, Jinlei Qi, Lijun Wang, and Maigeng Zhou. Long-term Fine Particulate Matter Exposure and Nonaccidental and Cause-specific Mortality in a Large National Cohort of Chinese Men. *Environmental Health Perspectives*, 125(11):117002, 2017. Publisher: Environmental Health Perspectives.

[26] Richard T. Burnett, Joseph V. Spadaro, George R. Garcia, and C. Arden Pope. Designing health impact functions to assess marginal changes in outdoor fine particulate matter. *Environmental Research*, 204:112245, 2022.

[27] NASA Socioeconomic Data and Applications Center (SEDAC). Gridded Population of the World, Version 4 (GPWv4): National Identifier Grid, 2018.

[28] Global Burden of Disease Collaborative Network. Global Burden of Disease Study 2021 (GBD 2021). Technical report, Institute for Health Metrics and Evaluation (IHME), Seattle, United States, 2024.

[29] Daniel Krewski, Michael Jerrett, Richard T. Burnett, Renjun Ma, Edward Hughes, Yuanli Shi, Michelle C. Turner, C. Arden Pope, George Thurston, Eugenia E. Calle, Michael J. Thun, Bernie Beckerman, Pat DeLuca, Norm Finkelstein, Kaz Ito, D. K. Moore, K. Bruce Newbold, Tim Ramsay, Zev Ross, Hwashin Shin, and Barbara Tempalski. Extended Follow-up and Spatial Analysis of the American Cancer Society Study Linking Particulate Air Pollution and Mortality. Research Report 140, Health Effects Institute, Boston, Mass, 2009.

[30] Johanna Lepeule, Francine Laden, Douglas Dockery, and Joel Schwartz. Chronic Exposure to Fine Particles and Mortality: An Extended Follow-up of the Harvard Six Cities Study from 1974 to 2009. *Environmental Health Perspectives*, 120(7):965–970, 2012.

[31] UNCTAD. UNCTAD STAT, 2024.

[32] Jose Nuno-Ledesma and Nelson B. Villoria. Estimating International Trade Margins Shares by Mode of Transport for the GTAP Data Base. *Journal of Global Economic Analysis*, 4(1):28–49, 2019. Number: 1.

[33] UNCTAD. *Review of Maritime Transport, 2018*. United Nations Conference on Trade and Development (UNCTAD), Geneva, Switzerland, 2018.

[34] IATA. Cargo, 2024.